Clinical extended-spectrum beta-lactamase antibiotic resistance plasmids have diverse transfer rates and can spread in the absence of antibiotic selection

Fabienne Benz[1*¶], Jana S. Huisman[1,2¶], Erik Bakkeren[3¶], Joana A. Herter[3], Tanja Stadler[2,4], Martin Ackermann[5,6], Médéric Diard[7], Adrian Egli[8,9&], Alex R. Hall[1&], Wolf-Dietrich Hardt[3&], Sebastian Bonhoeffer[1&]

[1]Institute of Integrative Biology, Department of Environmental Systems Science, ETH Zurich, Zurich, Switzerland

[2]Swiss Institute of Bioinformatics, Basel, Switzerland

[3]Institute of Microbiology, Department of Biology, ETH Zurich, Zurich, Switzerland

[4]Department of Biosystems Science and Engineering, ETH Zurich, Basel, Switzerland

[5]Institute of Biogeochemistry and Pollutant Dynamics, Department of Environmental Systems Science, ETH Zurich, Zurich, Switzerland

[6]Department of Environmental Microbiology, Eawag, Duebendorf, Switzerland

[7]Biozentrum, University of Basel, Basel, Switzerland

[8]Division of Clinical Bacteriology and Mycology, University Hospital Basel, Basel, Switzerland

[9]Applied Microbiology Research, Department of Biomedicine, University of Basel, Basel, Switzerland

[*] Corresponding author
E-mail: fabienne.benz@env.ethz.ch

[¶,&] These authors contributed equally to this work

Abstract

Horizontal gene transfer, mediated by conjugative plasmids, is a major driver of the global spread of antibiotic resistance. However, the relative contributions of factors that underlie the spread of clinically relevant plasmids are unclear. Here, we quantified conjugative transfer dynamics of Extended Spectrum Beta-Lactamase (ESBL) producing plasmids in the absence of antibiotics. We showed that clinical *Escherichia coli* strains natively associated with ESBL-plasmids conjugate efficiently with three distinct *E. coli* strains and one *Salmonella* enterica serovar Typhimurium strain, reaching final transconjugant frequencies of up to 1% within 24 hours *in vitro*. The variation of final transconjugant frequencies varied among plasmids, donors and recipients and was better explained by variation in conjugative transfer efficiency than by variable clonal expansion. We identified plasmid-specific genetic factors, specifically the presence/absence of transfer genes, that influenced final transconjugant frequencies. Finally, we investigated plasmid spread within the mouse intestine, demonstrating qualitative agreement between plasmid spread *in vitro* and *in vivo.* This suggests a potential for the prediction of plasmid spread in the gut of animals and humans, based on *in vitro* testing. Altogether, this may allow the identification of resistance plasmids with high spreading potential and help to devise appropriate measures to restrict their spread.

Introduction

Plasmids can transfer horizontally between bacterial cells of the same or of different species, thereby leading to rapid spread of accessory genes and allowing bacterial populations to adapt to new environments. Antibiotic resistance determinants are often plasmid-encoded and resistance plasmids drive the continuous rise of resistant bacterial pathogens that undermine the effectiveness of antibiotics in the clinic (1–3). Whether a plasmid can increase in frequency within a bacterial population depends on the plasmid as well as its bacterial host. Some plasmids become global threats in association with a specific clone (4–6). Other plasmids, however, are a clinical problem independent of their host strain (7). The family of Enterobacteriaceae is a key public health concern, as it includes some of the most important nosocomial pathogens and pandemic extended-spectrum beta-lactamases (ESBLs) producing strains (4,8–10). ESBLs provide their bacterial host with resistance to beta-lactam antibiotics, such as the widely used penicillins and cephalosporins, and are mostly encoded on plasmids of the incompatibility groups IncF and IncI (9,11,12).

In vitro studies revealed several key factors driving changes in plasmid frequency over time. For instance, if a plasmid of the same incompatibility group is already established in a potential recipient, plasmid incompatibility and surface- or entry exclusion may inhibit further plasmid acquisition (13,14). Some co-residing plasmids can enhance each other's stability (15) and allow or increase their transfer to a new bacterial host (16,17). Once a plasmid has been taken up by a bacterial cell, its replication system and the interaction with other host factors define whether it can be replicated and stably maintained. Bacterial immunity systems such as CRISPR, or a restriction modification system (RM system) different from the ones in the previous bacterial host, can eliminate an incoming plasmid (18–21). Whether a plasmid persists in a bacterial population over a longer time period depends on the frequency of plasmid loss during host replication (22) and the cost of plasmid carriage (23), although the latter can be reduced by the accumulation of compensatory mutations allowing for plasmid persistence (24). Such persistence can also occur when the cost of a plasmid in terms of a growth disadvantage is outperformed by its high rates of conjugation (25).

Save for a notable exception (26), these factors have mostly been studied separately from each other, with plasmids not directly relevant for antibiotic resistance spread or with

individual plasmids that have been moved into well-defined model strains (18,25,27). But to better understand the drivers of the spread of antibiotic resistance plasmids, we need to learn more about these factors' relative contributions to plasmid spread among clinical strains and in relevant environments. The gut of humans and farm animals contain a dense microbiota, which represent hotspots for bacterial interactions and transfer of antibiotic resistance plasmids. This knowledge relies on genomic studies (28–30) which, however, do not allow an investigation of the dynamics and drivers of plasmid spread. We, and others (31), have previously used mouse models to study processes that limit or boost plasmid spread in the gut (32–36). These studies, however, were limited to laboratory strains and single conjugative plasmids without clinical relevance, with the exception of one ESBL-plasmid used in (34). To our knowledge, there are no studies that compare plasmids and their transfer dynamics quantitatively *in vivo*.

Here, we use clinical *E. coli* strains and their natively associated ESBL-plasmids. We combine bioinformatic analyses with *in vitro* and *in vivo* experiments to provide a comprehensive and quantitative investigation of plasmid spread in the absence of antibiotic selection. Our *in vitro* conjugation experiments showed that the final frequencies of ESBL-plasmid carrying recipient strains (transconjugants) varied largely and were determined by plasmid, donor and recipient factors. The plasmid itself had the largest effect: Of the plasmids we tested, only those with functional transfer (*tra*) genes, including those encoding the sex pilus and the proteins required for the conjugative transfer (37–39), transferred to multiple recipients. None of the ESBL-plasmids lead to significant growth costs for recipient strains, neither *in vitro* nor *in vivo*. The plasmid frequency in recipient populations was determined by the rate at which they transferred horizontally to recipient strains (transfer rate). The rates of plasmid transfer varied depending on the donor-plasmid pair and the recipient strain. Importantly, our *in vitro* testing qualitatively predicted the plasmid spread in our antibiotic-free murine model for gut colonization. Furthermore, plasmid carriage was not associated with a cost in the gut and horizontal plasmid transfer determined the frequency of transconjugants. With this study, we contribute to connecting mechanisms of plasmid spread found *in vitro* with corresponding patterns *in vivo* and ultimately to a better understanding of the factors underlying the effective spread of clinically relevant resistance plasmids (5,40).

Materials and methods

Strains and growth conditions. We used 8 ESBL-plasmid positive *E. coli* strains as plasmid donors (D1-D8; Supplementary Table 1). They were sampled from patients in a transmission study at the University Hospital Basel, Switzerland, and their ESBL-plasmids reflect relevant vectors of ESBL mediated drug resistance (41). This collection comprised strains belonging to sequence types (ST) ST117, ST648, ST40, ST69, ST80, ST95, ST6697 and the very common ESBL sequence type ST131. We worked with 4 ESBL-plasmid negative recipient strains: RE1, a mouse-derived *E.coli* strain cured of its native IncI1 plasmid (35); RE2 and RE3, two clinical *E. coli* isolates from healthy patients (41,42); and RS1, the *Salmonella enterica* Typhimurium strain ATCC 14028 (RS). A comprehensive list of the plasmids found in these strains is given in Supplementary Table S1. Marker plasmids were introduced by electroporation, to mark recipients with either pACYC184 (New England Biolabs) encoding Chloramphenicol (Cm) resistance (except for RS, having chromosomal Cm resistance *marT::cat* (32)) or pBGS18 (43) encoding Kanamycin (Kan) resistance. Unless stated otherwise, we grew bacterial cultures at 37°C and under agitation (180 rpm) in lysogenic broth (LB) medium, supplemented with appropriate amounts of antibiotics (none, 100µg/mL Ampicillin (Amp), 25 µg/mL Cm *in vitro* and 15µg/mL Cm prior to *in vivo* experiments, 50µg/mL Kan). We stored isolates in 25% glycerol at -80°C.

Antibiotic resistance profiling. We used microdilution assays with a VITEK2 system (bioMérieux, France) to determine the minimum inhibitory concentrations (MIC). MIC breakpoints for ESBLs were interpreted according to EUCAST guidelines (v8.1). In addition, we confirmed resistance mechanism phenotypically, using ROSCO disk assays (ROSCO Diagnostica, Denmark), and/or genotypically with detection of CTX-M1 and CTX-M9 groups using the eazyplex Superbug assay (Amplex, Germany).

***In vitro* conjugation experiment.** We determined plasmid spread as the final frequency of the recipient population that obtained an ESBL-plasmid (transconjugants/(recipients+ transconjugants), T/(R+T)) in a high throughput, 96-well plate-based assay. Donor and recipient populations grew over night with or without Amp, respectively. We washed the independent overnight cultures by spinning down and resuspending and added ~1µL of 6.5-fold diluted donor and recipient cultures into 150µL fresh LB with a pin replicator (total ~1000-

fold dilution, aiming to reach approximately a 1:1 ratio of donor and recipient). These mating populations grew for 24 hours in the absence of antibiotics and were only shaken prior to hourly optical density (OD) measurements (Tecan NanoQuant Infinite M200 Pro). To determine the final cell densities, we plated the mating cultures at the end of the conjugation assay on selective LB-plates. In the first conjugation experiment, referred to as the 1st generation *in vitro* experiment, where the clinical strains transferred their native plasmids to recipients, we selected for donors+transconjugants with Amp, for recipients+transconjugants with Cm (*E. coli* recipients carried pACYC184-Cm and RS chromosomal *marT::cat*) and for transconjugants with Amp+Cm. For a second conjugation experiment, referred to as the 2nd generation *in vitro* experiment, we chose a subset of transconjugants generated in the 1st generation *in vitro* experiment as new plasmid donors. Transconjugants and recipients of the clone type RE3 were omitted because of the size of the experiment, and transconjugant RE2 carrying p1B_IncI had to be excluded as plasmid donor due to insufficient freezer stocks. We selected for donors with Cm, for recipients with Kan (recipients carried pBGS18-Kan) and for transconjugants with Kan+Amp. With this approach, we were able to detect transconjugant populations if their fraction exceeded 10^{-8} cells /mL. We performed experiments with *E. coli* recipients and *S.* Typhimurium recipient RS as independent experiments and the 1st generation *in vitro* (*n=4-6*) and 2nd generation *in vitro* (*n=6*) experiments each in two replica blocks.

The plasmids in our conjugation experiments could potentially be horizontally transferred either in the liquid mating population or after plating on selective plates (surface-mating). To assess the extent of surface-mating we performed an additional experiment, where we treated donors and recipients as above but grew them separate liquid cultures, instead of mixed cultures, only mixing them immediately before plating on selective LB-plates. To compare plasmid spread of 1st generation and 2nd generation *in vitro* experiments side by side, we performed a conjugation experiment as described above with D1 (with and without pACYC184) and transconjugants RE1 and RS carrying plasmid 1B_IncI, isolated from the 1st generation *in vitro* experiment, as plasmid donors.

***In vitro* plasmid cost experiment and other growth rate measurements.** To investigate the effect of ESBL-plasmid carriage on bacterial growth in absence of antibiotics, we measured the growth rate of transconjugants and recipients. Per donor and recipient combination, we

used three transconjugants, four replicates each, obtained from independent mating populations of the 1st generation *in vitro* experiment. Transconjugants for which we have not stored three independent transconjugants were excluded from this analysis. We grew bacterial cultures in absence of antibiotics overnight and diluted them 150-fold by transfer with a pin replicator to a 96-well plate, containing 150µL fresh LB per well. We incubated the cultures without shaking and estimated growth rates of recipients and transconjugants based on ten manual OD measurements over 24 hours. We estimated growth rates (h^{-1}) using the R package Growthcurver (44). We expressed plasmid cost as the growth rate of transconjugants relative to the corresponding ESBL-plasmid free recipient. Transconjugants have experienced longer growth under laboratory conditions than recipients (conjugation experiment). To verify that this did not affect our estimates of plasmid cost, we conducted a third growth rate experiment. First, recipients were grown under the same conditions as in the conjugation experiment but in absence of donor strains. Second, the growth rate of these treated strains was compared to the growth rates of untreated recipients (Supplementary Figure S1).

Other growth rate measurements (Supplementary Figures S1, S16) were performed as follows: We grew bacterial cultures with appropriate antibiotics overnight, washed and diluted them ~1000-fold. For the growth measurements, bacteria grew in the absence of antibiotics and the plate reader measured OD every hour for 24 hours. Again we estimated growth rates (h^{-1}) using the R package Growthcurver (44).

***In vivo* experiments.** We have previously established a murine model for enterobacterial pathogen infection (45) that allows to detect plasmid spread (32–36). For conjugation experiments, we used 8-16 week old C57BL/6 mice that contain an oligo microbiota allowing colonization of approximately 10^8 *E. coli* per gram faeces (46). *E. coli* stool densities of up to 10^8 cfu/g have also been detected in healthy human volunteers (42). We infected 7-10 mice per treatment group (minimum of two independent experiments; no antibiotic pre-treatment) orogastrically with ~$5x10^7$ CFU of RE2 or RE3, carrying marker plasmid pACYC184 and 24 hours later with ~$5x10^7$ CFU of either D4, D7, or D8. Faeces were collected daily, homogenized in 1 ml of PBS with a steel ball by a Tissue Lyser (Qiagen) at 25 Hz for 1 min. We enumerated bacterial populations by selective plating on MacConkey media (selection for donors+transconjugants with Amp (100 µg/mL), for recipients+transconjugants with Cm (15

202 µg/mL) and for transconjugants with Amp+Cm) and calculated final transconjugant
203 frequencies T/(R+T).

204 For competition experiments we infected 8-16-week-old C57BL/6 oligo microbiota mice
205 orogastrically with a 1:1 mixture of both competitor strains (~$5x10^7$ CFU total; no antibiotic
206 pre-treatment). We collected faeces and enumerated bacterial populations daily. We plated
207 bacteria on MacConkey agar containing Cm and replica-plated on media containing Cm, Kan,
208 and Amp to select the transfer deficient transconjugants. A change in fitness conferred by
209 plasmid carriage is reflected in the relative frequency of recipients to transconjugants (R/T).

210 Prior to all infections, we subcultured the overnight cultures (LB containing the appropriate
211 antibiotics) for 4 hours at 37°C without antibiotics (1:20 dilution) to ensure equal densities of
212 bacteria. Cells were washed in PBS and introduced into mice. All infection experiments were
213 approved by the responsible authority (Tierversuchskommission, Kantonales Veterinäramt
214 Zürich, license 193/2016 and license 158/2019).

215 **Sequencing, assembly, annotation**. We sequenced all donor and recipient strains with
216 Illumina MiSeq (paired end, 2x250 bp), Oxford Nanopore MinION and PacBio Sequel methods.
217 We produced hybrid assemblies with Unicycler (47) (v0.4.7) and used the most contiguous
218 assemblies (Oxford Nanopore – Illumina for D1,D2,D4,D6,D7,D8 and Pacbio Sequel – Illumina
219 for D3,D5, RE1, RE2, RE3). Manual curation involved removing contigs smaller than 1kB, and
220 sequences up to 5 kB that mapped to the own chromosome. We performed quality control
221 by mapping the paired end Illumina reads to the finished assemblies using samtools (v1.2)
222 and bcftools (v1.7) (48,49). For recipient RS, the ancestral strain was sequenced with Illumina
223 (2x150 bp), and mapped against the reference sequence, downloaded from NCBI Genbank
224 under the accession numbers NZ_CP034230.1 and NZ_CP034231.1.

225 To study the genetic contribution to the observed variation in plasmid spread, we sequenced
226 various transconjugants from the 1st and 2nd generation *in vitro* experiments as well as the *in*
227 *vivo* transfer experiment (Supplementary Table S2). *In vitro*: three clones from independent
228 mating populations for RE3 carrying plasmid p4A_IncI or p8A_IncF and one clone for the other
229 transconjugants. *In vivo*: eight clones of RE3 carrying p4A_IncI isolated from five mice on day
230 7 post donor infection, and eight clones of RE3 carrying p8A_IncF isolated from six mice on

231 day 2 (1 clone), day 6 (3 clones), or day 7 (4 clones) post donor infection. Resequencing was
232 performed on an Illumina MiSeq (paired end, 2x150 bp) and we mapped the reads to the
233 closed assemblies of respective donor and recipient strains using the breseq pipeline (v
234 0.32.0) (50). Mutations or indels shared by all re-sequenced strains were treated as ancestral
235 (Supplementary Table S2).

236 To investigate the transfer of plasmid p8C_IncBOKZ, we screened 3-5 transconjugants from
237 independent mating populations per conjugation pair (Supplementary Table S2). We
238 performed PCRs with primers specific to IncB/O and IncK plasmids (51), (5' to 3'):
239 MRxeBO_K_for: GAATGCCATTATTCCGCACAA and MRxeBO_K _rev; GTGATATACAGACCAT-
240 CACTGG).

241 To extract a chromosomal alignment of the *E. coli* donor and recipient strains, we
242 concatenated the genes returned by core genome Multi-Locus Sequence Typing (cgMLST) for
243 all strains. We used the chewBBACA software to type all strains according to the Enterobase
244 cgMLST scheme (52,53). We inferred the phylogenetic tree using BEAST2 (54), with an HKY
245 substitution model, a fixed mutation rate (fixed to the *E. coli* mutation rate of 10^{-4} mutations
246 per genome per generation, as estimated by Wielgoss et al. (55)), and a birth-death tree prior
247 (priors are listed in Supplementary Table S4). We performed bacterial genome annotation
248 using Prokka (56), and determined the sequence type (ST) using mlst (Torsten Seemann,
249 https://github.com/tseemann/mlst), which makes use of the PubMLST website
250 (https://pubmlst.org/) developed by Keith Jolley (57). Phylogroups were assigned using
251 ClermonTyper (58).

252 We determined genomic features using a range of bioinformatic tools, and by BLAST
253 comparison against various curated databases. Plasmid replicons and resistance genes were
254 identified using abricate (Torsten Seemann, https://github.com/tseemann/abricate) with the
255 PlasmidFinder (59) and ResFinder (60) databases respectively. We located phages using
256 PHASTER (61) (listing only those marked as "complete"), type 6 secretion systems using
257 SecReT6 (62), virulence genes using the Virulence finder database (63), toxin-antitoxin
258 systems using the database TADB 2.0 (64), and CRISPR-Cas loci using CRISPRCasFinder (65).
259 We found restriction-modification (RM) systems using grep on the term 'restriction' in the
260 general feature format (GFF) files from prokka, and verified them with the RM-database

261 Rebase (66). To determine the presence/absence of IncF and IncI transfer genes, we
262 constructed our own database as a reference. IncF transfer genes were taken from the
263 supplementary material of Fernandez-Lopez et al. (67), IncI1 transfer genes from plasmids
264 R64 using the annotations by Komano et al. (37), and Inc1γ transfer genes from the plasmid
265 R621a annotated by Takahashi et al. (38).

266 **Construction of non-transferrable plasmids**. For the *in vivo* competition experiments,
267 we generated non transferrable plasmids for three independent transconjugants. We deleted
268 their origin of transfer (*oriT*) region using the lambda red recombinase system with pKD4 as
269 template for the Kan resistance marker (68). The following primers were used (5' to 3'): For
270 IncI plasmids (p4A_IncI) DIncI_oriTnikA_f (GCATAAGACTATGATGCACAAAAATAAC-
271 AGGCTATAATGGGTGTAGGCTGGAGCTGCTTC) and DIncI_oriTnikA_r (CCTTCTCTTTTTCG-
272 GAATGACTGCATTCACCGGAGAATCCATGGGAATTAGCCATGGTCC) (35) and for F plasmids
273 (p8A_IncF) D25_2_oriT-nikA-ko_vw (CCATGATATCGCTCTCAGTAAATCCGGGTCTATTTTGTA-
274 AGTGTAGGCTGGAGCTGCTTC) and D25_2_oriT-nikA-ko-rev (GTGCGGACACAGACTGGATATTT-
275 TGCGGATAAAATAATTTATGGG-AATTAGCCATGGTCC). We verified all mutants by PCR
276 (IncI1_oriT _val_f: AGTTCCTCA-TCGGTCATGTC, IncI1_oriT _val_r: GAAGCCATTGGCACTTTCTC,
277 D25_oriT _val_fw: CATACAGG-GATCTGTTGTC and D25_2_oriT_ver_rv: CAGAATCACTAT-
278 TCTGACAC) and experimentally by loss of transfer function.

279 **Statistical analyses.** For *in vitro* experiments we performed analyses using R (version 3.4.2).
280 The effects of donor, recipient and plasmid on final transconjugant frequency were analyzed
281 with either a two-way ANOVA (1st generation *in vitro* experiment with factors donor-plasmid
282 pair and recipient) or a three-way ANOVA (2nd generation *in vitro* experiment with factors
283 donor, plasmid, recipient). For the 1st generation *in vitro* experiment, we excluded strain-
284 plasmid pairs which did not result in transconjugants (D2, D3, D7) and recipient RS from this
285 analysis. When single replicates for a given donor-recipient combination lacked
286 transconjugants (D5 and D6), we assigned these replicates a final transconjugant frequency
287 at the detection limit of 10^{-8}. With the same data we performed the correlation of final
288 transconjugant frequency and transfer rate. The data of the 2nd generation *in vitro* experiment
289 was not fully factorial. To enable testing of interactions, we therefore performed two 3-way
290 ANOVAs: one excluding plasmid p1B_IncI and one excluding donor RE2, for which we had to

take the two replicate blocks into account: $P < 0.001$). For two replicate populations (RS self-self transfer with p1B_IncI), we had higher counts on plates selecting for transconjugants than on plates selecting for recipients+transconjugants and replaced the resulting negative CFU/mL for recipients with 0 CFU/mL (we assume the higher count on selective agar reflects measurement error, given the true frequency of plasmid-carrying cells cannot exceed 1.0). We used the end-point method of Simonsen *et al.* to determine plasmid transfer rates in diverse bacterial populations (69).

For statistical comparisons derived from *in vivo* experiments, Kruskal-Wallis tests were performed with Dunn's multiple test correction using GraphPad Prism Version 8 for Windows.

300 **Results**

301 Strains and plasmids. We used eight clinical E. coli strains as ESBL-plasmid donors (D1-D8) and
302 four recipient strains susceptible to β-Lactam antibiotics, of which three are E. coli (RE1-RE3)
303 and one S. Typhimurium (RS, Supplementary Figure S2, Supplementary Table S3). Sequence
304 analysis revealed a large phylogenetic diversity, with donor strains belonging to phylogenetic
305 groups B1, B2, D or its subgroup F, and recipients to either B2 or A (Figure 1). We also
306 observed diverse accessory traits such as bacterial immunity systems (Supplementary Figure
307 S3) and virulence genes (Supplementary Figure S4). All but two strains encode type 6
308 secretion systems (T6SS), and strain D4 shows an Enteropathogenic (EPEC) virulence profile.
309 Each strain carries at least one and up to eight plasmids of various incompatibility groups
310 (Supplementary Figure S5, Table S1). Every donor strain harbours a single antibiotic-
311 resistance plasmid (the ESBL plasmid), either of the plasmid family IncI or IncF (Table 1) and
312 displayed an ESBL-resistance phenotype (Supplementary Table S3). All strains encode
313 numerous intact prophage sequences in their chromosome (Supplementary Figure S6) and
314 we found P1-like phages, i.e. prophages that move like plasmids in their lysogenic phase
315 (70,71), in various strains (Supplementary Figure S7). ESBL-plasmid p2A_IncF carries a SPbeta-
316 like prophage (68.4 kB), which encodes all 12 resistance genes of that plasmid. With the
317 exception of p3A_crypt and pRE3B_crypt, all plasmids bigger than 35 kB carry plasmid
318 addiction systems (22) (toxin-antitoxin (TA) systems, Supplementary Figure S8).

319 **Diverse clinical ESBL-plasmids spread extensively through recipient populations in the**
320 **absence of antibiotics.** To investigate the spread of ESBL-plasmids in the absence of
321 antibiotics, we first performed conjugation experiments with all possible donor-recipient
322 combinations (referred to as 1st generation *in vitro* experiment). We use the final
323 transconjugant frequency, i.e. the fraction of the recipient population that carried the ESBL-
324 plasmid after 24 hours, to measure plasmid spread. The highest final transconjugant
325 frequency (~0.1%) was achieved when plasmid p4A_IncI spread in populations of recipient
326 RE3. Five of the eight ESBL-plasmids spread in more than one of the *E. coli* recipients and their
327 final transconjugant frequencies spanned 5 orders of magnitude (Figure 2A). The average final
328 transconjugant frequency varied depending on the donor-plasmid pair and among recipient
329 strains (two-way ANOVA excluding D2, D3, D7, effect of donor-plasmid pair: $F_{4,66}$ = 87.665,
330 P < 0.01, effect of recipient: $F_{2,66}$ = 5.439, P < 0.01). The variation among donor-plasmid pairs

331 depended also on the recipient (donor-plasmid pair×recipient interaction: $F_{8,66}$ = 3.164,
332 P < 0.01). Although these ESBL-plasmids are natively associated with *E. coli*, they reached
333 comparable maximal transconjugant frequencies in the RS (i.e. *S*. Typhimurium) recipient
334 populations (Figure 2B). The variation across donor-plasmid pairs was similar to that obtained
335 with *E. coli* recipients, with the exception of p6A_IncI, which did not spread to recipient RS.

336 The pili of type IncI and IncF plasmids support plasmid transfer on solid surface and in liquid
337 growth environment (72). To investigate to which extent these ESBL-plasmids could transfer
338 after plating on selective plates, we performed a surface-mating experiment for a subset of
339 donor-recipient combinations (Supplementary Figure S9). On this solid surface, only p1B_IncI
340 and p4A_IncI transferred from donor to recipient and resulted in transconjugant frequencies
341 ranging from 10^{-8} to 10^{-5}, in a recipient-dependent manner (two-way ANOVA excluding D6,
342 D8 and RS: effect of recipient: $F_{2,18}$ = 34.29, effect of donor-plasmid pair: $F_{1,18}$ = 13.750, P <
343 0.01 in both cases). This suggests that most of the plasmid transfer in our conjugation
344 experiments took place in the liquid growth environment.

345 **Plasmid, donor and recipient factors lead to variation in plasmid spread.** In the 1st
346 generation *in vitro* experiment (Figure 2), each plasmid was present in a single donor and thus
347 we could not separate the contributions of plasmid and donor strain to the observed plasmid
348 spread. Therefore, we performed an second conjugation experiment (referred to as 2nd
349 generation *in vitro* experiment) under conditions identical to the 1st generation *in vitro*
350 experiment, but where each donor strain was represented with multiple different plasmids
351 and each plasmid was represented in multiple donors. Specifically, for the 2nd generation *in*
352 *vitro* experiment, we used eight transconjugants isolated from the 1st generation *in vitro*
353 experiment as plasmid donors and three of the same recipient strains (Figure 3). The final
354 transconjugant frequency varied among donor strains and among plasmids (three-way
355 ANOVA with plasmid, excluding p1B_IncI, donor and recipient as factors, effect of donor
356 strain: $F_{2,90}$ = 150.133, P < 0.001, effect of plasmid: $F_{1,90}$ = 49.717, P < 0.001). Variation among
357 plasmids depended on both, the recipient and the donor strain (donor strain×plasmid
358 interaction: $F_{2,90}$ = 96.352, P < 0.001; recipient×plasmid interaction: $F_{2,90}$ = 29.610, P < 0.001).
359 For instance, when the donor and recipient strains were both RS, both IncI ESBL-plasmids
360 yielded remarkably high final transconjugant frequencies of 40%. A second analysis supported
361 variation among donor strains and plasmids and that variation among plasmids depended on

362 recipient and donor strain (three-way ANOVA excluding RE2, effect of donor strain: $F_{1,93}$ =
363 560.269, $P < 0.001$, effect of plasmid $F_{2,93}$ = 156.075, $P < 0.001$, recipient×plasmid interaction:
364 $F_{4,93}$ = 26.104, $P < 0.001$, donor strain×plasmid interaction: $F_{2,93}$ = 3.999, P = 0.022). As in our
365 1st generation *in vitro* experiment, average final transconjugant frequencies also varied
366 among recipients ($P < 0.001$ for effect of recipient in both three-way ANOVAs). Thus, the final
367 frequency of transconjugants depended on donor strain, plasmid, and recipient. Also, we
368 found plasmid spread to be especially efficient when donor and recipient are the same strain
369 (Figure 3, self-self transfer).

370 For some plasmid-recipient combinations we noticed that replacing the native donor strains
371 with transconjugants from the 1st generation *in vitro* assay (primary and secondary plasmid
372 transfer, respectively) led to large differences in final transconjugant frequencies (Figures 2
373 and 3). For a subset of strains, we tested whether these resulted solely from the substitution
374 of the native donor strain (D1) with a secondary plasmid host (RE1 and RS, Supplementary
375 Figure S12). When RE1 and RS acted as a donor strain for plasmid p1B_IncI, transconjugant
376 frequencies of RE1 carrying p1B_IncI increased 45-fold and 112-fold, respectively, compared
377 to when p1B_IncI was transferred from its native donor strain D1. When both donor and
378 recipient were RS, the final transconjugant frequency increased 2800-fold compared to
379 transfer of plasmid p1B_IncI from its native host D1 to RS. Indeed, this showed that plasmid
380 transfer from a secondary bacterial host can differ strongly from its transfer from the initial
381 host.

382 **ESBL-plasmids can spread rapidly *in vivo*, with efficiencies correlating with the *in vitro***
383 **trends.** Transfer of ESBL-plasmids in the human gut has only been confirmed by sequence-
384 based studies (28,73). However, to our knowledge the dynamics of their spread *in vitro* have
385 not yet been thoroughly compared to any *in vivo* system. Therefore, we performed
386 conjugation experiments over seven days in absence of antibiotics. These were done in
387 gnotobiotic mice with a defined microbiota (46), with three clinical donors (D4, D8, and D7),
388 and two recipients (RE2 and RE3, Figure 4). The residential microbiota allows colonization of
389 approximately 10^8 *E. coli* per gram faeces, *E. coli* densities representative of the guts of some
390 humans and animals (42,74). The variation of ESBL-plasmid spread *in vivo* was in qualitative
391 agreement with the 1st generation *in vitro* experiment. As in the 1st generation *in vitro*
392 experiment (Figure 2) for recipient RE3 we observed highest transconjugant frequencies with

plasmid p4A_IncI followed by p8A_IncF and no transconjugants with p7A_IncF (Figure 4). Furthermore, the final transconjugant frequency with plasmid p4A_IncI was higher with RE3 than RE2 both *in vivo* and *in vitro* (see Figure 4A-B, blue dots, and Figure 2). Lastly, the final transconjugant frequencies with p8A_IncF were similar for both recipient populations (Figure 4A-B, purple dots, and Figure 2). Because the final frequency of RE3 carrying p4A_IncI (1%) was already reached at day 1, we re-performed this conjugation experiment, sampling more densely in time and found the final transconjugant frequency to be established already eight hours after the orogastric introduction of donor D4 (Supplementary Figure S13). This rapid increase in transconjugant frequency was followed by a 6-day plateau, which may result from the simultaneous decrease of recipient and transconjugant populations over time (Supplementary Figure S14). Indeed, direct competition experiments *in vivo* (Supplementary Figure S15) confirmed the competitive advantage of donor D4 over RE3. This fitness benefit can perhaps be explained by the difference in *in vitro* growth rate estimates (Supplementary Figure S16).

ESBL-plasmids generate no significant cost after transfer to new bacterial hosts *in vitro* and *in vivo*. We investigated the effect of plasmids on bacterial growth in the absence of antibiotics for ten strain-plasmid combinations *in vitro*. We estimated plasmid cost as the growth rate of transconjugants relative to their respective plasmid-free recipient strain and found no significant effect of plasmid carriage (Figure 5A-B, Student's t-Test for *E. coli* hosts and Wilcoxon Rank Sum Test for *S.* Typhimurium, $P > 0.05$ in all cases, before and after Holm's correction for multiple testing). *In vivo*, we investigated the effect of ESBL-plasmids p4A_IncI and p8A_IncF on bacterial fitness with direct 1:1 competition between recipient RE3 and its transconjugants (Figure 5C). After seven days of competition, for transconjugants with p4A_IncI, there was no significant change in the relative frequency of recipients to transconjugants. Transconjugants carrying p8A_IncF outcompeted RE3 leading to a relative frequency of ~0.1 after seven days, indicating a minor fitness advantage by carriage of p8A_IncF.

Plasmid transfer rates drive plasmid spread and their *in vitro* estimates are a good proxy for *in vivo* transfer. The observed variation in final transconjugant frequencies *in vitro* and the dynamics in the mouse gut could be driven by horizontal plasmid transfer or by clonal expansion of transconjugants. Although non-significant, *in vitro,* the *S*. Typhimurium

transconjugants showed a consistent trend towards higher relative growth rates (Figure 5B). Our calculations demonstrated that differences in growth rates resulting from ESBL-plasmid carriage could indeed explain final transconjugant frequencies of *S.* Typhimurium recipients carrying p1B_IncI and p8A_IncF, but not plasmid spread in any *E. coli* recipient population (Supplementary Results). To estimate plasmid transfer rates, we applied the Simonsen method to population densities obtained in the 1st generation *in vitro* experiment (S3 Table) (69). We found that conjugative transfer rates of primary transfer, from donor to recipient, correlate strongly with observed final transconjugant frequencies, across all donor-recipient combinations (Supplementary Figure S17, Pearson's test, $r = 0.99$, $P < 0.001$). Together, this suggests that horizontal plasmid transfer from donor to recipient dictated observed spread of ESBL-plasmids *in vitro*.

The *in vivo* competition experiment revealed a growth advantage of RE3 when carrying p8A_IncF, allowing a two-fold increase of the initial transconjugant frequency when growing for seven days in the gut (from 0.5 to 0.9, Figure 5C). Because we used *oriT*-mutants, no plasmid could be horizontally transferred during this competition experiment and therefore increasing transconjugant populations must have resulted from clonal growth. Allowing for horizontal plasmid transfer (seven-day conjugation experiment), however, the transconjugant frequency of RE2 and RE3 carrying p8A_IncF increased from the detection limit of 10^{-6} up to final frequencies of 1% (Figure 4A-B). This large difference in transconjugant population increase with and without conjugation allows us to conclude that in our gut colonization model without antibiotic selection, the spread of ESBL-plasmids was driven by conjugative transfer, rather than by clonal expansion of transconjugants. The fast increase of the transconjugant population RE3 carrying p4A_IncI within only eight hours (Supplementary Figure S13), despite a lack of growth advantage over recipient RE3 (Figure 5C), further supports this result. *In vitro*, we found that transfer from donor strains and from transconjugants to recipient strains could vary several orders of magnitude (Supplementary Figure S12). Such a difference in primary and secondary plasmid transfer could also be present *in vivo*. However, the transconjugant populations were minor compared to the size of the donor populations throughout the *in vivo* experiment (Supplementary Figure S14). Thus, we can conclude that most transfer events were between donors and recipients, rather than between transconjugants and recipients. Altogether, we showed horizontal transfer to allow

455 for rapid ESBL-plasmid spread in the murine gut, in the absence of antibiotic selection, and
456 demonstrated that our *in vitro* transfer rates reflect *in vivo* transfer dynamics.

457 **Plasmid factors are the main determinant of observed plasmid transfer rates.** We
458 demonstrated that the extent of the spread of ESBL-plasmids in both *in vitro* and *in vivo*
459 systems was a result of their transfer rates. To investigate genetic factors that might influence
460 plasmid transfer rates, we performed detailed bioinformatic analyses on plasmids, donor and
461 recipient genomes. We found that the presence of essential *tra* genes on ESBL-plasmids is the
462 main genomic factor predicting their spread (Figure 6): the 5/8 ESBL-plasmids encoding all
463 necessary *tra* genes spread to at least three of the five recipient strains.

464 Our experiments showed that the more fine-scale variation in plasmid spread depends on
465 donor and recipient factors (Figures 2-3). We investigated whether the phylogenetic
466 relatedness of strains (Figure 1) could explain observed plasmid transfer dynamics.
467 Qualitatively, the relatedness of mating donor and recipient strains was not correlated with
468 transfer rates: D5 and D6 are equally closely related to recipients RE1 and RE2, yet we
469 observed very different final transconjugants frequencies (Figure 2). Additionally, recipient RS
470 is phylogenetically distant to all the donors, yet we observed variation in final transconjugants
471 frequency similar to those observed across *E. coli* recipients. In contrast, the relatedness of
472 plasmids with regard to their replicons, because plasmids carrying the same replicon can pose
473 a barrier to each other, seemed to be a good predictor of plasmid spread. The final
474 transconjugant frequencies of the IncFII ESBL-plasmids p5A_IncF and p6A_IncI/F varied
475 largely depending on recipients (Figure 2). They were highest with recipient RE1, likely
476 because it is the only recipient without a plasmid encoding an IncFII-replicon. The lack of
477 transconjugants resulting from conjugation of donor D6 carrying plasmid p6A_IncI/F with
478 recipient RS, could be due to the incompatibility with the resident plasmid pRS_IncF. This is
479 intriguing because the presence of *tra* genes (Figure 6) indicates that plasmid p6A_IncI/F
480 transfers with the IncI1 transfer machinery, whereas the incompatibility can only be IncFII
481 based.

482 We sequenced transconjugants resulting from both *in vitro* and the *in vivo* conjugation
483 experiments (Supplementary Table S2). This provided further evidence for the role of
484 incompatibility. Plasmid p8A_IncF carries half of the IncFIC-FII replicon (Supplementary Figure

485 S5) and resulted in the loss of the resident F-plasmid pRE3A_IncF in recipient RE3, both *in*
486 *vitro* and *in vivo*. This plasmid interference, however, seemed not to limit the transfer of
487 plasmid p8A_IncF into RE3, because it spread to all recipients at the same rate (Figure 2).

488 Donor and recipient strains carry multiple non-ESBL plasmids that could have been
489 transferred during conjugation experiments. Sequencing revealed only a few isolated cases
490 of co-transferring plasmids *in vitro* and none *in vivo*. For plasmid p8C_IncBOKZ we found some
491 transfer to all four recipients of the 1st generation experiment and from there even to further
492 recipients in the 2nd generation experiment. This process seemed independent of donor and
493 recipient strains (Supplementary Table S2). The only small Col-plasmids that were transferred
494 were p1D_ColRNAI and p8G_Col8282. The P1 phage-like plasmid p8B_p0111 transferred *in*
495 *vitro* to RE3 but not *in vivo* (Supplementary Table S2). Although they encode the *tra* genes (S2
496 File), the resident plasmids in the recipients (RE2, RE3 and RS) showed no horizontal transfer.
497 Sequencing transconjugants also allowed us to screen for mutations that could explain some
498 of the variation in final transconjugant frequencies across donor-recipient pairs or between
499 primary and secondary plasmid transfer (Figures 2-3). We found no mutations on ESBL-
500 plasmids, neither after the 24-hours *in vitro* nor the 7-days *in vivo* conjugation experiments
501 (Supplementary Table S2). The only consistent changes on plasmids were the mutations of P1
502 phage-like plasmid p8B_p0111, which was passed to recipient RE3 *in vitro,* but not *in vivo*:
503 here we found mutations in the genomic region encoding side tail fibre proteins. Similar
504 mutations were also frequently present within chromosomal prophages. We found several
505 other chromosomal mutations in transconjugants (Supplementary Table S2). For instance, all
506 transconjugants resulting from conjugation into RE1 recipients (*n = 11*) and some (*n = 9* out
507 of 22) RE3 recipients showed intergenic mutations in the promoter sequence or the phase
508 ON/OFF region of the *fim* operon. The *fim* genes encode the type 1 pilus (type 1 fimbria), a
509 virulence factor responsible for cell adherence (75). RE1 chromosomally encodes for two
510 mobilization proteins mobA, required for the mobilization of plasmid and conjugative
511 transposons. In all 11 sequenced RE1-transconjugants, we found various intergenic mutations
512 upstream of at least one *mobA*.

513 We found various RM systems (Supplementary Figure S3) and investigated whether ESBL-
514 plasmid transfer from an RM deficient donor into a recipient with this RM system could
515 explain reduced plasmid transfer rates. We found high rates of self-self transfer (Figure 3),

which could result from identical RM systems in donor and recipient strains but for other mating pairs, we found no relation between RM systems and transfer rates. The anti-restriction protein YfjX (ardB) is present in nearly all strains, including on all ESBL-plasmids, and could reduce the detrimental effect of RM systems in recipients. We found the adaptive immunity systems CRISPR-Cas Type 1F (recipients RE1 and RE2) and CRISPR-Cas Type 1E (recipients RE3, RS and donors D1-4, D8). We investigated whether they could be a barrier to conjugation, by screening whether the spacer sequences in recipient strains matched any of our plasmids or phages. This was not the case. We further investigated the activity of the CRISPR system *in vitro* and *in vivo* by screening all CRISPR arrays in sequenced transconjugants for spacer sequences that were not present in the recipients prior to conjugation. We did not observe spacer acquisition, neither *in vitro* nor *in vivo*.

Discussion

Conjugative plasmids are a key driver of the antibiotic resistance crisis through their ability to spread within and between bacterial species. Many possible factors affecting their spread have been identified, but most studies investigate these factors *in vitro*, in laboratory strains or in isolation (13–15,27,76). Understanding the relevance of these factors in ecologically complex environments, where plasmid transfer typically occurs, necessitates studies that aim to untangle their relative contributions. Here we combined bioinformatic analyses with *in vitro* and *in vivo* experiments and provide a comprehensive and quantitative investigation of plasmid spread in the absence of antibiotic selection.

We found that differences in horizontal plasmid transfer and not cost of plasmid carriage are the main source of variation in plasmid spread. In this study, ESBL-plasmids encoding the essential genes for conjugation spread efficiently and the variation of their spread depended also on recipient and donor strain. This is of particular importance because approximately half of all known plasmids can transfer via conjugation (16) and thus, a substantial amount of antibiotic resistance plasmids have the potential to spread through diverse bacterial populations without the need for strong selective forces, such as antibiotics.

Our measurements of plasmid spread *in vitro* showed good qualitative agreement with plasmid spread in a mouse model, which was reflected in the ranking of final transconjugant frequencies and its dependence on the recipient strain. This suggests that key aspects of

546 plasmid spread in complex environments can be quantified with higher throughput *in vitro*
547 testing. *In vivo*, the rise of the transconjugant frequency was remarkably fast. RE3 carrying
548 plasmid p4A_IncI reached a frequency of 1% after 8 hours, but surprisingly plateaued
549 thereafter. Explanations thereof could be the outcompetition of recipient and transconjugant
550 populations by the plasmid donor strain or a reduced growth rate after initial colonization of
551 the plasmid donor strain. The latter one, however, seems unlikely as we would expect this to
552 lead to a similar pattern for D8. Alternatively, this could result from spatial heterogeneities of
553 bacterial populations. A high initial plasmid transfer rate with a plateau after one day has
554 previously been observed for biofilm assays and in a streptomycin-treated mouse model (77)
555 and was attributed to the fixed spatial position of donor and recipient cells in the biofilm and
556 the mucus layer of the gut, respectively. We found that on a solid surface, p4A_IncI spread at
557 100-fold higher rates in RE3 than RE2 recipient populations, suggesting that plasmid transfer
558 with recipient RE3 could benefit from a structured environment. In the colonization model
559 used for our conjugation experiments (45), such interactions of bacteria with the host
560 intestinal lining could also allow for more structured populations (78), and may indeed result
561 in the observed transfer dynamics of plasmid p4A_IncI.

562 In natural systems bacteria often harbour multiple plasmids, which affect their ability to
563 acquire further plasmids. Using bioinformatic analyses, we studied various plasmid features
564 and related those to observed plasmid spread. We found plasmid incompatibility to play a
565 role in conjugation with ST131 strains D5 and D6, but also to be a permeable barrier. This
566 might be explained by the multiple replicons encoded on ESBL-plasmids, a strategy to
567 circumvent limitations in spread due to plasmid incompatibility (79). Co-transfer of other
568 plasmids has also been proposed to affect plasmid transfer rates (80), but we found little
569 plasmid co-transfer and could not relate its occurrence to observed plasmid spread.
570 Sequencing of the ESBL-plasmids in transconjugants revealed no mutations after transfer. This
571 is in agreement with earlier findings reporting the absence of mutations on ESBL-plasmids
572 even after 112 days of evolution of transconjugants (81). This suggests that clinical ESBL-
573 plasmids are well adapted to Enterobacteriaceae and do not require clone-specific
574 adaptations for successful spread.

575 Using bioinformatic analysis we also studied how strain-specific features influence plasmid
576 spread. We found that all four recipient strains encode the adaptive immunity system CRISPR-

577 Cas Type I, of which Type IF (recipients RE1 and RE2) is commonly associated with
578 antimicrobial susceptibility in *E. coli* (82). It is generally believed that in laboratory *E. coli*
579 strains such as K12, Type I CRISPR-Cas loci are inactive under laboratory growth conditions
580 (83). This was also suggested by our investigation of spacer acquisition. Other bacterial
581 defence systems are also known to affect the efficiency of plasmid transfer (84). For instance,
582 it has been proposed that plasmid transfer to close kin is more efficient due to the similarity
583 in RM systems of donor and recipient strains (27). Here, however, we did not find this relation.
584 The ESBL-plasmids used in this study employ anti-restriction strategies like many other
585 conjugative plasmids (85), and thus, we and others suggest that RM systems may only
586 marginally shape horizontal plasmid transfer in natural systems (86,87).

587 Given the central role of plasmids in the spread of antibiotic resistance, it is of great
588 importance to understand the factors contributing to plasmid spread under natural
589 conditions. Studies focusing on well-defined plasmid and laboratory strains have identified
590 multiple factors relevant for plasmid spread under laboratory conditions. How these factors
591 play together to affect plasmid spread under natural conditions, is key to understand why
592 clinically relevant combinations of bacterial strains and plasmids, such as *E. coli* ST131 with
593 IncFII plasmids encoding $bla_{\text{CTX-M}}$, have become global threats (4–6). Encouragingly, the
594 qualitative agreement between the *in vitro* measurements and the plasmid spread in the
595 mouse model, suggests that *in vitro* testing with relevant clinical strains and plasmids may
596 potentially be a good proxy for plasmid spread also in humans. Linking large-scale *in vitro*
597 conjugation experiments using clinically relevant plasmid-strain combinations with
598 epidemiological information on their spread thus seems an important avenue of future
599 research to delineate the factors contributing to the global spread of antibiotic resistance by
600 plasmids.

601 **Competing Interests**

602 The authors declare no conflict of interest.

603 **Acknowledgements**

604 We would like to acknowledge the members of the Bonhoeffer, Hall, Hardt, Diard, Egli,
605 Stadler, and Ackermann labs, as well as Sebastien Wielgoss, for helpful discussions. We would
606 also like to thank the staff at the RCHCI and EPIC animal facilities at ETH Zurich, particularly

Sven Nowok; as well as the NGS team and Dr. Daniel Wuethrich of the Clinical Bacteriology and Mycology department at the University Hospital Basel for their excellent technical support. This work was funded by the NRP72 SNF grant (407240-167121) to SB, AH, AE, MA, TS and WDH. Additionally, AE, WDH and SB were supported by the Gebert Rüf Foundation "Microbials" programme grant "displacing ESBL", EB by the Boehringer Ingelheim Fonds PhD Fellowship and MD by the SNSF professorship grant PP00PP_176954.

References

1. Sommer MOA, Munck C, Toft-Kehler RV, Andersson DI. Prediction of antibiotic resistance: Time for a new preclinical paradigm? Nat Rev Microbiol. 2017;15(11):689–96.
2. Pitout JD, Laupland KB. Extended-spectrum β-lactamase-producing Enterobacteriaceae: an emerging public-health concern. Lancet Infect Dis. 2008 Mar 1;8(3):159–66.
3. Cassini A, Högberg LD, Plachouras D, Quattrocchi A, Hoxha A, Simonsen GS, et al. Attributable deaths and disability-adjusted life-years caused by infections with antibiotic-resistant bacteria in the EU and the European Economic Area in 2015: a population-level modelling analysis. Lancet Infect Dis. 2019;19(1):56–66.
4. Davies J, Davies D. Origins and Evolution of Antibiotic Resistance. Microbiol Mol Biol Rev. 2010;74(3):1092–2172.
5. San Millan A. Evolution of Plasmid-Mediated Antibiotic Resistance in the Clinical Context. Trends Microbiol. 2018;26(12):978–85.
6. Dunn SJ, Connor C, McNally A. The evolution and transmission of multi-drug resistant Escherichia coli and Klebsiella pneumoniae: the complexity of clones and plasmids. Curr Opin Microbiol. 2019 Oct;51:51–6.
7. Poirel L, Potron A, Nordmann P. OXA-48-like carbapenemases: The phantom menace. J Antimicrob Chemother. 2012;67(7):1597–606.
8. Bajaj P, Singh NS, Virdi JS. Escherichia coli β-Lactamases: What Really Matters. Front Microbiol. 2016 Mar 30;7:417.
9. Carattoli A. Resistance plasmid families in Enterobacteriaceae. Antimicrob Agents Chemother. 2009;53(6):2227–38.
10. Roca I, Akova M, Baquero F, Carlet J, Cavaleri M, Coenen S, et al. The global threat of antimicrobial resistance: science for intervention. New Microbes New Infect. 2015;6:22–9.
11. Paterson DL, Bonomo RA. Extended-spectrum beta-lactamases: a clinical update. Clin Microbiol Rev. 2005 Oct;18(4):657–86.
12. Rozwandowicz M, Brouwer MSM, Fischer J, Wagenaar JA, Gonzalez-Zorn B, Guerra B, et al. Plasmids carrying antimicrobial resistance genes in Enterobacteriaceae. J

Antimicrob Chemother. 2018;73(5):1121–37.
13. Frost LS, Ippen-Ihler K, Skurray3 RA. Analysis of the Sequence and Gene Products of the Transfer Region of the F Sex Factor. Microbiol Rev. 1994;5(2):162–210.
14. Garcillán-Barcia MP, de la Cruz F. Why is entry exclusion an essential feature of conjugative plasmids? Vol. 60, Plasmid. 2008. p. 1–18.
15. San Millan A, Heilbron K, MacLean RC. Positive epistasis between co-infecting plasmids promotes plasmid survival in bacterial populations. ISME J. 2014;8(3):601–12.
16. Smillie C, Garcillan-Barcia MP, Francia M V., Rocha EPC, de la Cruz F. Mobility of Plasmids. Vol. 74, Microbiology and Molecular Biology Reviews. 2010. p. 434–52.
17. Dionisio F, Zilhão R, Gama JA. Interactions between plasmids and other mobile genetic elements affect their transmission and persistence. Plasmid. 2019 Feb;
18. Purdy D, O'Keeffe TAT, Elmore M, Herbert M, McLeod A, Bokori-Brown M, et al. Conjugative transfer of clostridial shuttle vectors from Escherichia coli to Clostridium difficile through circumvention of the restriction barrier. Mol Microbiol. 2002 Oct;46(2):439–52.
19. Thomas CM, Nielsen KM. Mechanisms of, and barriers to, horizontal gene transfer between bacteria. Vol. 3, Nature Reviews Microbiology. 2005. p. 711–21.
20. Doron S, Melamed S, Ofir G, Leavitt A, Lopatina A, Keren M, et al. Systematic discovery of antiphage defense systems in the microbial pangenome. Science (80-). 2018;359(6379):0–12.
21. Price VJ, Mcbride SW, Hullahalli K, Chatterjee A, Duerkop BA, Palmer KL. Enterococcus faecalis CRISPR-Cas Is a Robust Barrier to Conjugative Antibiotic Resistance Dissemination in the Murine Intestine. 2019;
22. Hayes F. Toxins-Antitoxins: Plasmid Maintenance, Programmed Cell Death, and Cell Cycle Arrest. Science (80-). 2003;301(5639):1496–9.
23. San Millan A, MacLean RC. Fitness Costs of Plasmids: a Limit to Plasmid Transmission. Microbiol Spectr. 2017;5(5).
24. Harrison E, Guymer D, Spiers AJ, Paterson S, Brockhurst MA. Parallel Compensatory Evolution Stabilizes Plasmids across the Parasitism-Mutualism Continuum. Curr Biol. 2015;25(15):2034–9.
25. Lopatkin AJ, Meredith HR, Srimani JK, Pfeiffer C, Durrett R, You L. Persistence and

reversal of plasmid-mediated antibiotic resistance. Nat Commun. 2017;

26. Hardiman CA, Weingarten RA, Conlan S, Khil P, Dekker JP, Mathers AJ, et al. Horizontal transfer of carbapenemase-encoding plasmids and comparison with hospital epidemiology data. Antimicrob Agents Chemother. 2016;60(8):4910–9.

27. Dimitriu T, Marchant L, Buckling A, Raymond B. Bacteria from natural populations transfer plasmids mostly towards their kin. Proc R Soc B Biol Sci. 2019;286(1905).

28. Knudsen PK, Gammelsrud KW, Alfsnes K, Steinbakk M, Abrahamsen TG, Müller F, et al. Transfer of a bla CTX-M-1-carrying plasmid between different Escherichia coli strains within the human gut explored by whole genome sequencing analyses. Sci Rep. 2018;8(1):280.

29. Liebana E, Batchelor M, Hopkins KL, Clifton-Hadley FA, Teale CJ, Foster A, et al. Longitudinal farm study of extended-spectrum beta-lactamase-mediated resistance. J Clin Microbiol. 2006 May 1;44(5):1630–4.

30. Stoesser N, Sheppard AE, Moore CE, Golubchik T, Parry CM, Nget P, et al. Extensive within-host diversity in fecally carried extended-spectrum-beta-lactamase-producing Escherichia coli Isolates: Implications for transmission analyses. J Clin Microbiol. 2015;53(7):2122–31.

31. Ott LC, Stromberg ZR, Redweik GAJ, Wannemuehler MJ, Mellata M. Mouse Genetic Background Affects Transfer of an Antibiotic Resistance Plasmid in the Gastrointestinal Tract. mSphere. 2020 Jan 29;5(1).

32. Diard M, Bakkeren E, Cornuault JK, Moor K, Hausmann A, Sellin ME, et al. Inflammation boosts bacteriophage transfer between *Salmonella* spp. Science (80-). 2017;355(6330):1211–5.

33. Moor K, Diard M, Sellin ME, Felmy B, Wotzka SY, Toska A, et al. High-avidity IgA protects the intestine by enchaining growing bacteria. Nature. 2017;544(7651):498–502.

34. Bakkeren E, Huisman JS, Many O, Bonhoeffer S, Regoes RR, Diard M, et al. Salmonella persisters promote the spread of antibiotic resistance plasmids in the gut. Nature. 2019;573:276–280.

35. Stecher B, Denzler R, Maier L, Bernet F, Sanders MJ, Pickard DJ, et al. Gut inflammation can boost horizontal gene transfer between pathogenic and commensal Enterobacteriaceae. Proc Natl Acad Sci. 2012;109(4):1269–74.

36. Wotzka SY, Kreuzer M, Maier L, Arnoldini M, Nguyen BD, Brachmann AO, et al. Escherichia coli limits Salmonella Typhimurium infections after diet shifts and fat-mediated microbiota perturbation in mice. Vol. 4, Nature Microbiology. 2019. p. 2164–74.
37. Komano T, Yoshida T, Narahara K, Furuya N. The transfer region of IncI1 plasmid R64: Similarities between R64 tra and Legionella icm/dot genes. Mol Microbiol. 2000;35(6):1348–59.
38. Takahashi H, Shao M, Furuya N, Komano T. The genome sequence of the incompatibility group Iγ plasmid R621a: Evolution of IncI plasmids. Plasmid. 2011;66(2):112–21.
39. Koraimann G. Spread and Persistence of Virulence and Antibiotic Resistance Genes: A Ride on the F Plasmid Conjugation Module. EcoSal Plus. 2018;8(1).
40. MacLean RC, Millan AS. The Evolution of Antibiotic Resistance. Science (80-). 2019;365(6458):1082–3.
41. Tschudin-Sutter S, Frei R, Schwahn F, Tomic M, Conzelmann M, Stranden A, et al. Prospective Validation of Cessation of Contact Precautions for Extended-Spectrum beta-Lactamase-Producing Escherichia coli. Emerg Infect Dis. 2016;22(6):1094–7.
42. Wotzka SY, Kreuzer M, Maier L, Zünd M, Schlumberger M, Nguyen B, et al. Microbiota stability in healthy individuals after single-dose lactulose challenge—A randomized controlled study. Staley C, editor. PLoS One. 2018 Oct 25;13(10):e0206214.
43. Spratt BG, J. Hedge P, Heesen S te, Edelman A, Broome-Smith JK. Kanamycin-resistant vectors that are analogues of plasmids pUC8, pUC9, pEMBL8 and pEMBL9. Gene. 1986 Jan 1;41(2–3):337–42.
44. Sprouffske K, Wagner A. Growthcurver: an R package for obtaining interpretable metrics from microbial growth curves. BMC Bioinformatics. 2016 Dec 19;17(1):172.
45. Barthel M, Hapfelmeier S, Quintanilla-Martínez L, Kremer M, Rohde M, Hogardt M, et al. Pretreatment of Mice with Streptomycin Provides a Salmonella enterica Serovar Typhimurium Colitis Model That Allows Analysis of Both Pathogen and Host. Infect Immun. 2003;71(5):2839–58.
46. Brugiroux S, Beutler M, Pfann C, Garzetti D, Ruscheweyh HJ, Ring D, et al. Genome-guided design of a defined mouse microbiota that confers colonization resistance against Salmonella enterica serovar Typhimurium. Nat Microbiol. 2016;2(2):1–12.

740 47. Wick RR, Judd LM, Gorrie CL, Holt KE. Unicycler: Resolving bacterial genome
741 assemblies from short and long sequencing reads. PLoS Comput Biol. 2017;13(6):1–
742 22.
743 48. Li H. A statistical framework for SNP calling, mutation discovery, association mapping
744 and population genetical parameter estimation from sequencing data. Bioinformatics.
745 2011;27(21):2987–93.
746 49. Li H, Handsaker B, Wysoker A, Fennell T, Ruan J, Homer N, et al. The Sequence
747 Alignment/Map format and SAMtools. Bioinformatics. 2009;25(16):2078–9.
748 50. Barrick JE, Colburn G, Deatherage DE, Traverse CC, Strand MD, Borges JJ, et al.
749 Identifying structural variation in haploid microbial genomes from short-read
750 resequencing data using breseq. BMC Genomics. 2014;15(1):1–17.
751 51. Compain F, Poisson A, Le Hello S, Branger C, Weill FX, Arlet G, et al. Targeting relaxase
752 genes for classification of the predominant plasmids in Enterobacteriaceae. Int J Med
753 Microbiol. 2014;304(3–4):236–42.
754 52. Silva M, Machado MP, Silva DN, Rossi M, Moran-Gilad J, Santos S, et al. chewBBACA:
755 A complete suite for gene-by-gene schema creation and strain identification. Microb
756 genomics. 2018;4(3):1–7.
757 53. Alikhan NF, Zhou Z, Sergeant MJ, Achtman M. A genomic overview of the population
758 structure of Salmonella. PLoS Genet. 2018;14(4):1–13.
759 54. Bouckaert R, Heled J, Kühnert D, Vaughan T, Wu CH, Xie D, et al. BEAST 2: A Software
760 Platform for Bayesian Evolutionary Analysis. PLoS Comput Biol. 2014;10(4):1–6.
761 55. Wielgoss S, Barrick JE, Tenaillon O, Cruveiller S, Chane-Woon-Ming B, Médigue C, et
762 al. Mutation Rate Inferred From Synonymous Substitutions in a Long-Term Evolution
763 Experiment With Escherichia coli. G3 Genes, Genomes, Genet. 2011;1(3):183–6.
764 56. Seemann T. Prokka: Rapid prokaryotic genome annotation. Bioinformatics.
765 2014;30(14):2068–9.
766 57. Jolley KA, Maiden MCJ. BIGSdb: Scalable analysis of bacterial genome variation at the
767 population level. BMC Bioinformatics. 2010;11.
768 58. Beghain J, Bridier-Nahmias A, Le Nagard H, Denamur E, Clermont O. ClermonTyping:
769 an easy-to-use and accurate in silico method for Escherichia genus strain phylotyping.
770 Microb Genomics. 2018;4(7):1–8.
771 59. Carattoli A, Zankari E, Garcia-Fernandez A, Larsen MV, Lund O, Villa L, et al. In Silico

detection and typing of plasmids using plasmidfinder and plasmid multilocus sequence typing. Antimicrob Agents Chemother. 2014;58(7):3895–903.

60. Zankari E, Hasman H, Cosentino S, Vestergaard M, Rasmussen S, Lund O, et al. Identification of acquired antimicrobial resistance genes. 2012;(July):2640–4.

61. Arndt D, Grant JR, Marcu A, Sajed T, Pon A, Liang Y, et al. PHASTER: a better, faster version of the PHAST phage search tool. Nucleic Acids Res. 2016;44(W1):W16–21.

62. Li J, Yao Y, Xu HH, Hao L, Deng Z, Rajakumar K, et al. SecReT6: A web-based resource for type VI secretion systems found in bacteria. Environ Microbiol. 2015;17(7):2196–202.

63. Joensen KG, Scheutz F, Lund O, Hasman H, Kaas RS, Nielsen EM, et al. Real-time whole-genome sequencing for routine typing, surveillance, and outbreak detection of verotoxigenic Escherichia coli. J Clin Microbiol. 2014;52(5):1501–10.

64. Xie Y, Wei Y, Shen Y, Li X, Zhou H, Tai C, et al. TADB 2.0: An updated database of bacterial type II toxin-antitoxin loci. Nucleic Acids Res. 2018;46(D1):D749–53.

65. Couvin D, Bernheim A, Toffano-Nioche C, Touchon M, Michalik J, Néron B, et al. CRISPRCasFinder, an update of CRISRFinder, includes a portable version, enhanced performance and integrates search for Cas proteins. Nucleic Acids Res. 2018;46(W1):W246–51.

66. Roberts RJ, Vincze T, Posfai J, Macelis D. REBASE-a database for DNA restriction and modification: Enzymes, genes and genomes. Nucleic Acids Res. 2015;43(D1):D298–9.

67. Fernandez-Lopez R, de Toro M, Moncalian G, Garcillan-Barcia MP, de la Cruz F. Comparative genomics of the conjugation region of F-like plasmids: Five shades of F. Front Mol Biosci. 2016 Nov 10;3(NOV):71.

68. Datsenko KA, Wanner BL. One-step inactivation of chromosomal genes in Escherichia coli K-12 using PCR products. Proc Natl Acad Sci U S A. 2000;97(12):6640–5.

69. Simonsen L, Gordon DM, Stewart FM, Levin BR. Estimating the rate of plasmid transfer: an end-point method. J Gen Microbiol. 1990;136(11):2319–25.

70. Samojedny a., Lobocka MB, Yarmolinsky MB, Lehnherr H, Plunkett G, Rose DJ, et al. Genome of Bacteriophage P1. J Bacteriol. 2004;186(21):7032–68.

71. Venturini C, Zingali T, Wyrsch ER, Bowring B, Iredell J, Partridge SR, et al. Diversity of P1 phage-like elements in multidrug resistant Escherichia coli. Sci Rep. 2019;9(1).

72. Trevor Lawley, Brian M. Wilkins LSF. Bacterial Conjugation in Gram-Negative Bacteria.

In: Plasmid biology. ASM Press; 2004. p. 203–26.

73. Conlan S, Park M, Deming C, Thomas PJ, Young AC, Coleman H, et al. Plasmid Dynamics in KPC-Positive Klebsiella pneumoniae during Long-Term Patient Colonization. MBio. 2016 Jun;7(3):e00742-16.

74. Tenaillon O, Skurnik D, Picard B, Denamur E. The population genetics of commensal Escherichia coli. Nat Rev Microbiol. 2010;8(3):207–17.

75. Schwan WR. Regulation of fim genes in uropathogenic Escherichia coli. World J Clin Infect Dis. 2011;1(1):17.

76. Finbarr H. Toxins-Antitoxins: Plasmid Maintenance, Programmed cell death in bacterial populations. Science. 1995 Feb 10;267(5199):836–7.

77. Licht TR, Christensen BB, Krogfelt KA, Molin S. Plasmid transfer in the animal intestine and other dynamic bacterial populations: The role of community structure and environment. Microbiology. 1999;145(9):2615–22.

78. Furter M, Sellin ME, Hansson GC, Hardt WD. Mucus Architecture and Near-Surface Swimming Affect Distinct Salmonella Typhimurium Infection Patterns along the Murine Intestinal Tract. Cell Rep. 2019 May 28;27(9):2665-2678.e3.

79. Villa L, García-Fernández A, Fortini D, Carattoli A. Replicon sequence typing of IncF plasmids carrying virulence and resistance determinants. J Antimicrob Chemother. 2010;65(12):2518–29.

80. Gama JA, Zilhão R, Dionisio F. Conjugation efficiency depends on intra and intercellular interactions between distinct plasmids: Plasmids promote the immigration of other plasmids but repress co-colonizing plasmids. Plasmid. 2017;93(August):6–16.

81. Mahérault AC, Kemble H, Magnan M, Gachet B, Roche D, Nagard H Le, et al. Advantage of the F2:A1:B- IncF Pandemic Plasmid over IncC Plasmids in in Vitro Acquisition and Evolution of blaCTX-M Gene-Bearing Plasmids in Escherichia coli. Antimicrob Agents Chemother. 2019;63(10):e01130-19.

82. Aydin S, Personne Y, Newire E, Laverick R, Russell O, Roberts AP, et al. Presence of Type I-F CRISPR/Cas systems is associated with antimicrobial susceptibility in Escherichia coli. J Antimicrob Chemother. 2017;72(8):2213–8.

83. Pougach K, Semenova E, Bogdanova E, Datsenko KA, Djordjevic M, Wanner BL, et al. Transcription, processing and function of CRISPR cassettes in Escherichia coli. Mol

Microbiol. 2010;77(6):1367–79.

84. Thomas CM, Nielsen KM. Mechanisms of, and barriers to, horizontal gene transfer between bacteria. Vol. 3, Nature Reviews Microbiology. 2005. p. 711–21.

85. Tock MR, Dryden DTF. The biology of restriction and anti-restriction. Vol. 8, Current Opinion in Microbiology. 2005. p. 466–72.

86. Liang W, Xie Y, Xiong W, Tang Y, Li G, Jiang X, et al. Anti-Restriction Protein, KlcAHS, Promotes Dissemination of Carbapenem Resistance. Front Cell Infect Microbiol. 2017 May 2;7.

87. Serfiotis-Mitsa D, Herbert AP, Roberts GA, Soares DC, White JH, Blakely GW, et al. The structure of the KlcA and ArdB proteins reveals a novel fold and antirestriction activity against type I DNA restriction systems in vivo but not in vitro. Nucleic Acids Res. 2009;38(5):1723–37.

Figure 1 **Phylogenetic tree of the *E. coli* donor and recipient strains, inferred using Bayesian inference on a core genome alignment.** Strain names at the tips are coloured by *E. coli* phylogroup. The *S*. Typhimurium recipient RS was not included in the phylogeny, but listed here to allow comparison of the plasmid content. RE1-3 denotes the three *E. coli* recipients and D1-8 denotes the eight donors. Blue rectangles show that a plasmid with the indicated IncF or IncI replicon (incompatibility marker) is present in that strain. A red dot indicates the replicon(s) present on the ESBL-plasmid in each strain.

Figure 2 **ESBL-plasmids spread at variable rates in the absence of antibiotics (1st generation *in vitro* experiment)**. Plasmid spread was measured as the final transconjugant frequency, i.e. the ratio of the recipient population carrying the ESBL-plasmid (T), relative to the total of plasmid-free (R) and plasmid carrying (T) recipient populations. Final transconjugant frequency is shown for recipient populations of *E. coli* strains RE1-3 (A) and *S*. Typhimurium strain RS (B). Circles represent independent replicates (n=4-6) and the beams are mean values ± standard error of the mean (SEM). The detection limit was at ~10^{-8}. Total population densities can be found in Supplementary Figure S10.

Figure 3 **Final transconjugant frequency depends on donor, recipient, and plasmid (2nd generation *in vitro* experiment).** Eight transconjugants isolated from mating assays in the 1st generation *in vitro* experiment (Figure 2), used here as plasmid donor strains, transferred their plasmid to three different recipients. Circles represent independent replicates (n = 6), the beams are mean values ± SEM and different plasmids are indicated in colour. The detection limit was at ~10^{-8}. Total population densities can be found in Supplementary Figure S11. Donor RE2 carrying plasmid p1B_IncI was excluded, see methods.

Figure 4 **ESBL-plasmids can spread in the gut in the absence of antibiotic selection.** We measured the spread of three plasmids as final transconjugant frequency in two distinct recipient populations, A) RE2 and B) RE3, and enumerated transconjugants in faeces by selective plating. Dotted lines indicate the detection limit for selective plating. Circles represent independent replicates (n = 7 for RE2 conjugations; n =7 for D4-RE3; n = 10 for D8-RE3 and D7-RE3), lines show the median and different donor-plasmid pairs are indicated in colour. Kruskal-Wallis test p>0.05 (ns), p<0.05 (*), p<0.01 (**), p<0.001 (***), p<0.0001 (****). Total population densities can be found in Supplementary Figure S14.

Figure 5 **No evidence for cost of plasmid carriage for transconjugants.** A-B) We measured plasmid cost for ten strain-plasmid combinations, with three independently isolated transconjugants each (n = 4; beams are mean values ± SEM). Transconjugants and their plasmid free complements grew in independent cultures and we calculated the relative growth by dividing the transconjugant growth rates (h^{-1}) by the mean growth-rate of plasmid-free strains. C) We performed the competition experiment by colonizing the mice with a 1:1 mix of a non-conjugative transconjugant (*oriT*-knockout) and recipient RE3 (n = 6; 3 independent transconjugants, n = 2 for each). (C) Kruskal-Wallis test p>0.05 (ns), p<0.01 (**).

Figure 6 **Transfer genes**. Presence (blue) or absence (white) of essential *tra* genes for IncF plasmids (A), and IncI plasmids (B). Genes and panels in grey are non-essential for pilus biogenesis, DNA transfer or conjugation,

884 according to Koraiman (39) (A) and Komano (37,38) (B). ESBL-plasmids are indicated by an asterisk: green
885 indicates spread to multiple recipient populations, orange indicates conjugation with only one replicate
886 population, and red indicates no transfer. Non-ESBL plasmids are labelled in black. Plasmid p6A_IncI/IncF is
887 shown on both panels A and B, but only the IncI1 transfer system is complete.

Figure 1

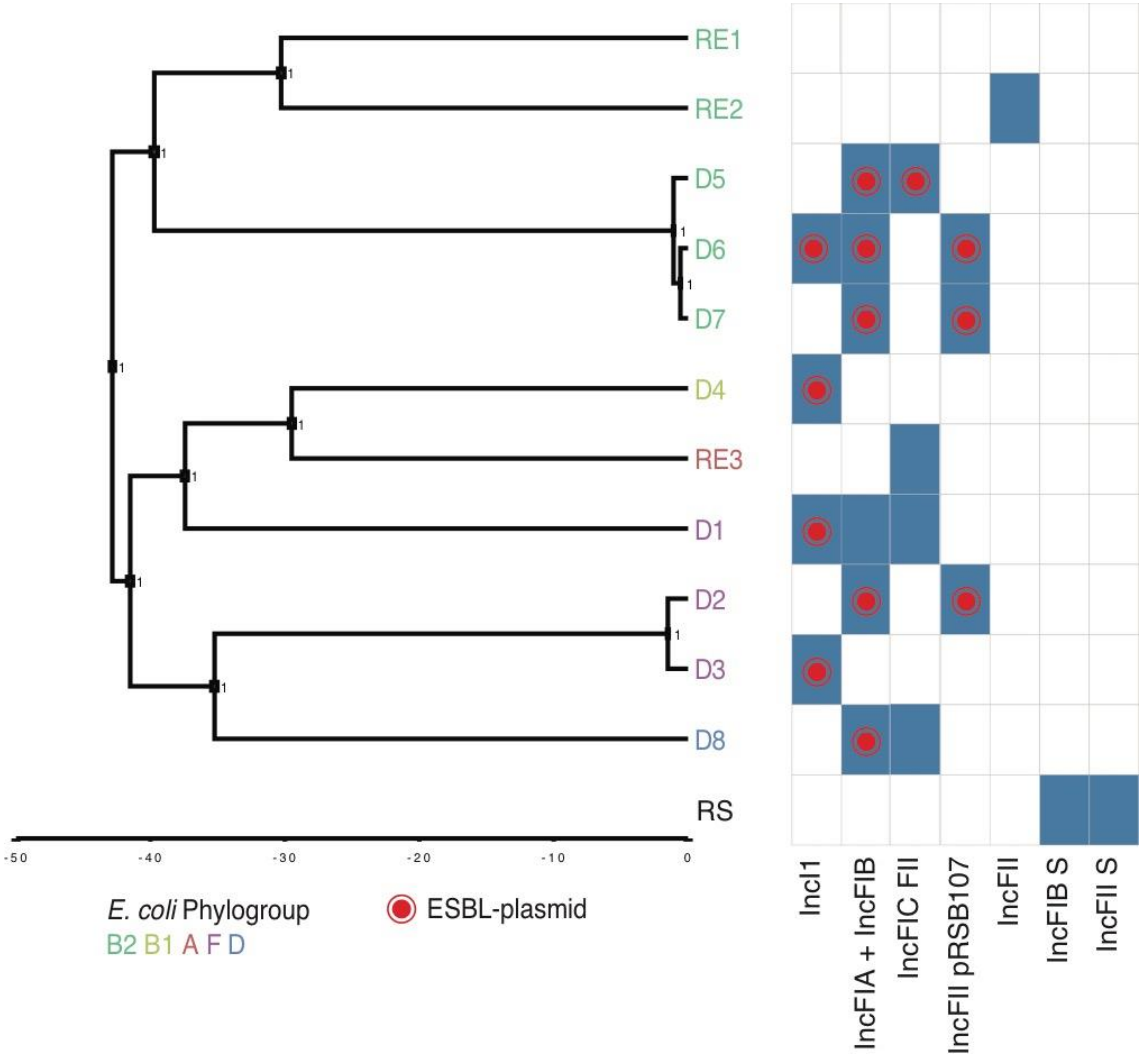

Figure 2

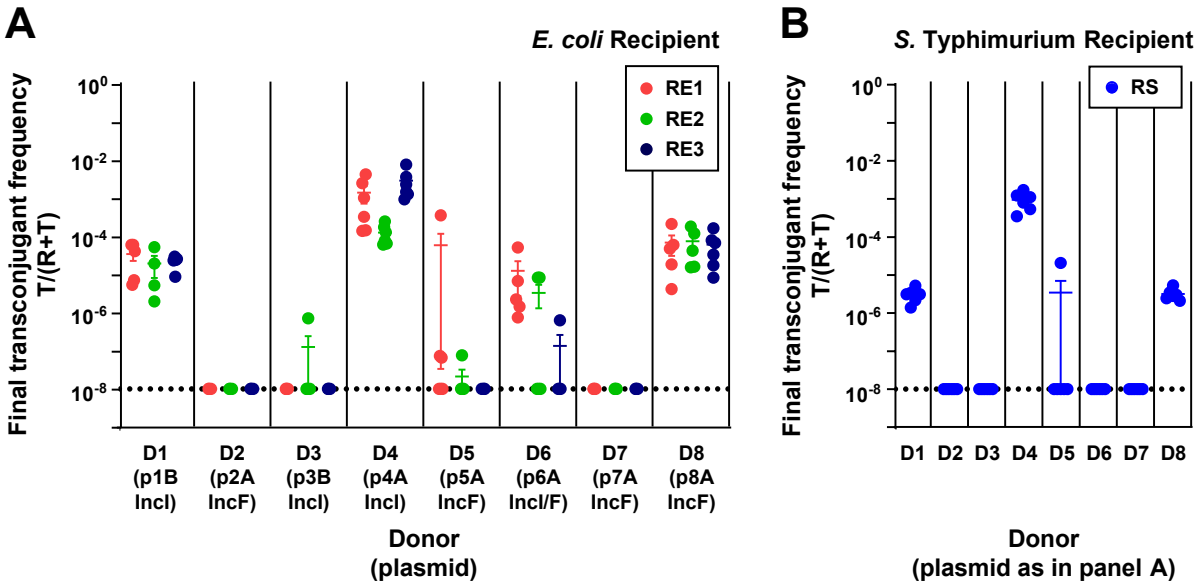

Figure 3

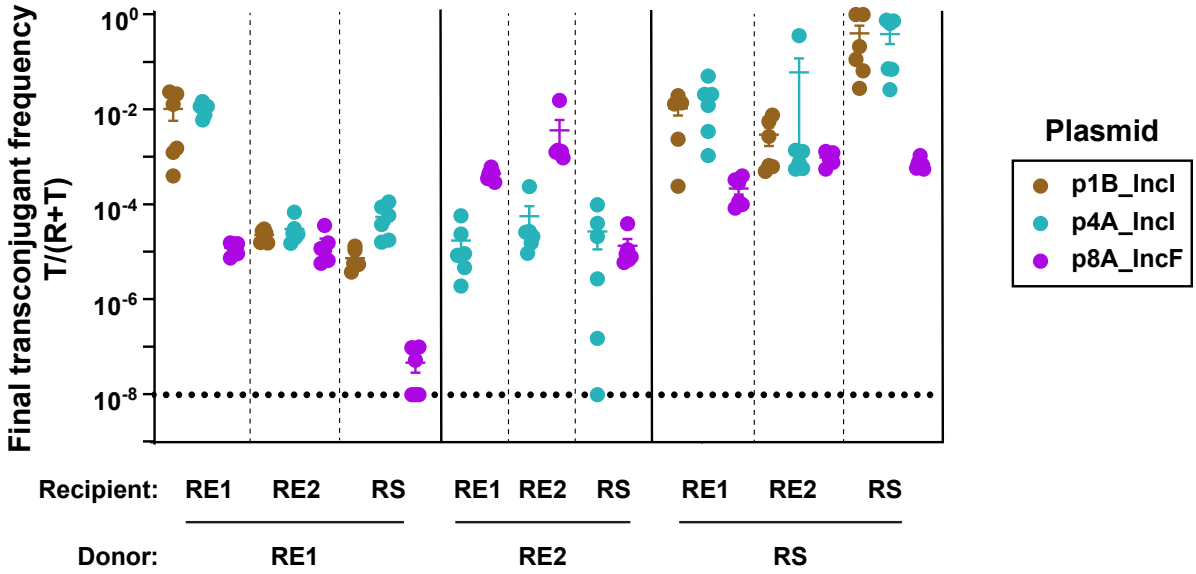

Figure 4

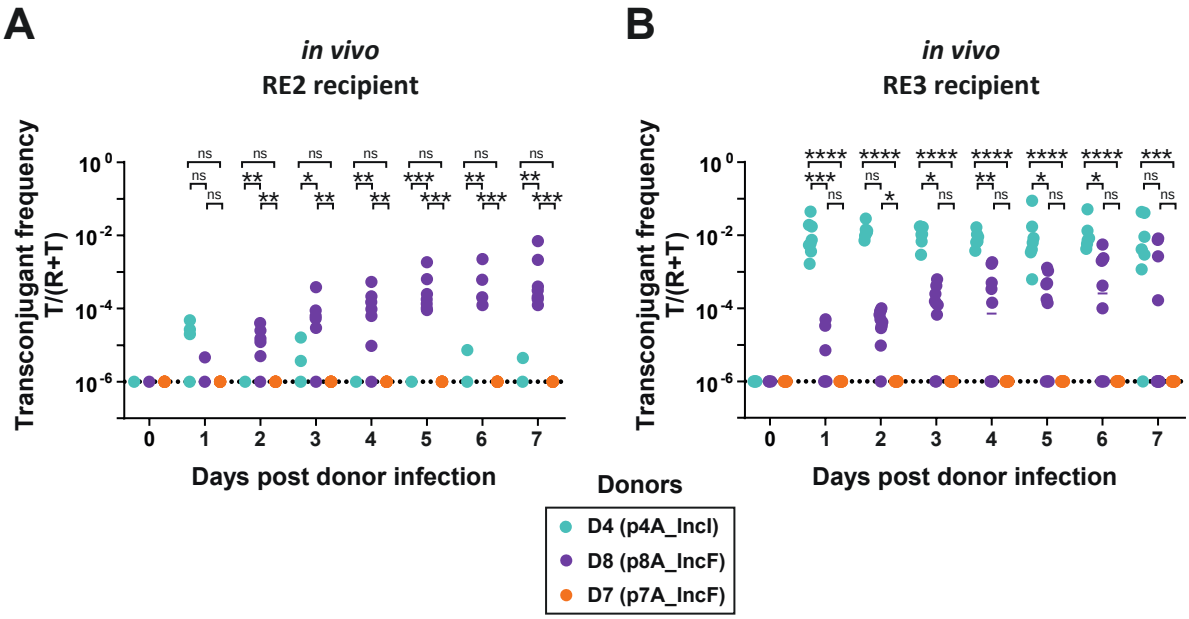

Figure 5

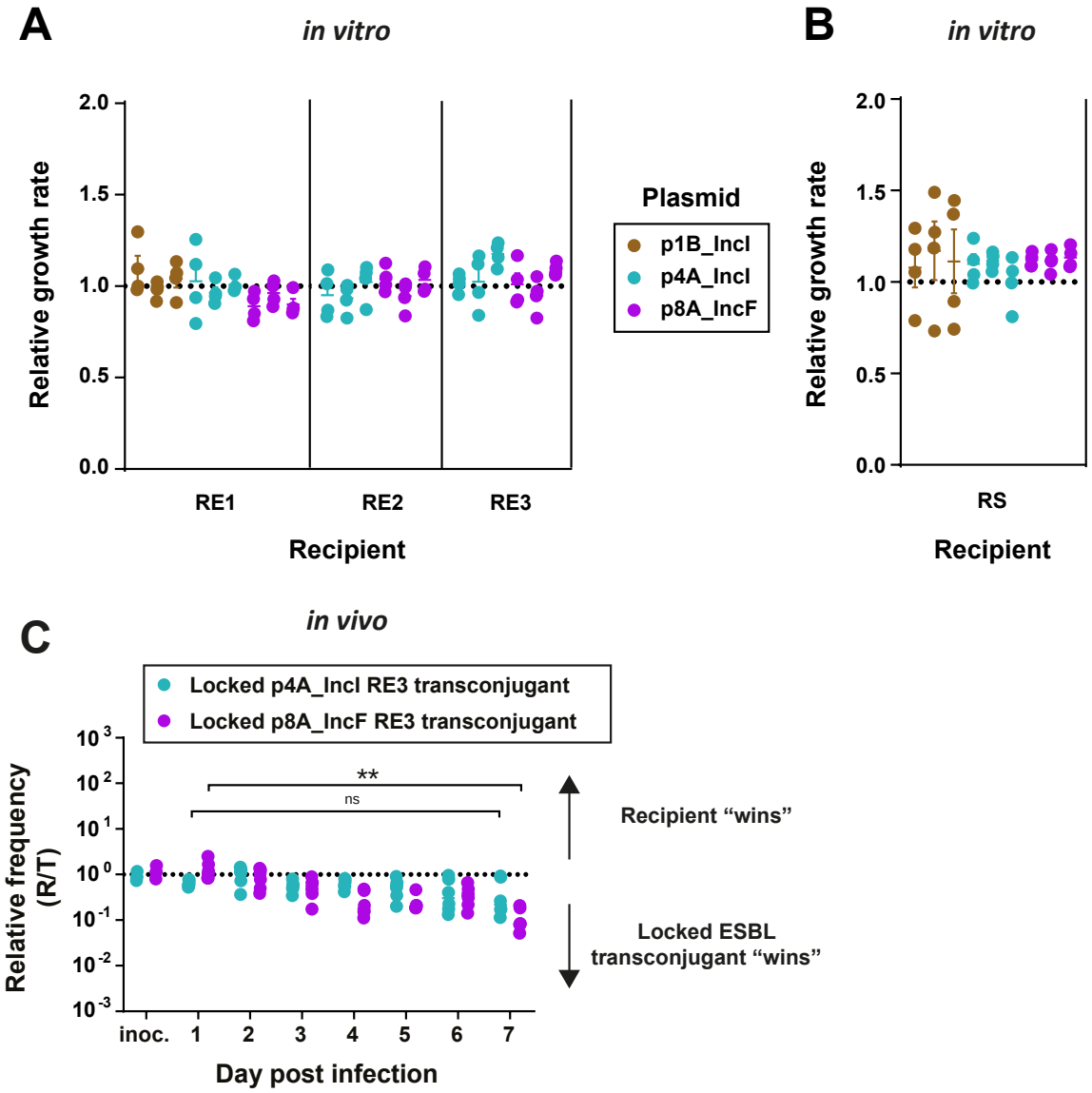
A
in vitro
Relative growth rate
2.0
1.5
1.0
0.5
0.0
RE1
RE2
RE3
Recipient
Plasmid
p1B_IncI
p4A_IncI
p8A_IncF
B
in vitro
Relative growth rate
2.0
1.5
1.0
0.5
0.0
RS
Recipient
C
in vivo
Locked p4A_IncI RE3 transconjugant
Locked p8A_IncF RE3 transconjugant
Relative frequency (R/T)
10 3
10 2
10 1
10 0
10 -1
10 -2
10 -3
**
ns
Recipient "wins"
Locked ESBL transconjugant "wins"
inoc.
1
2
3
4
5
6
7
Day post infection

Figure 6

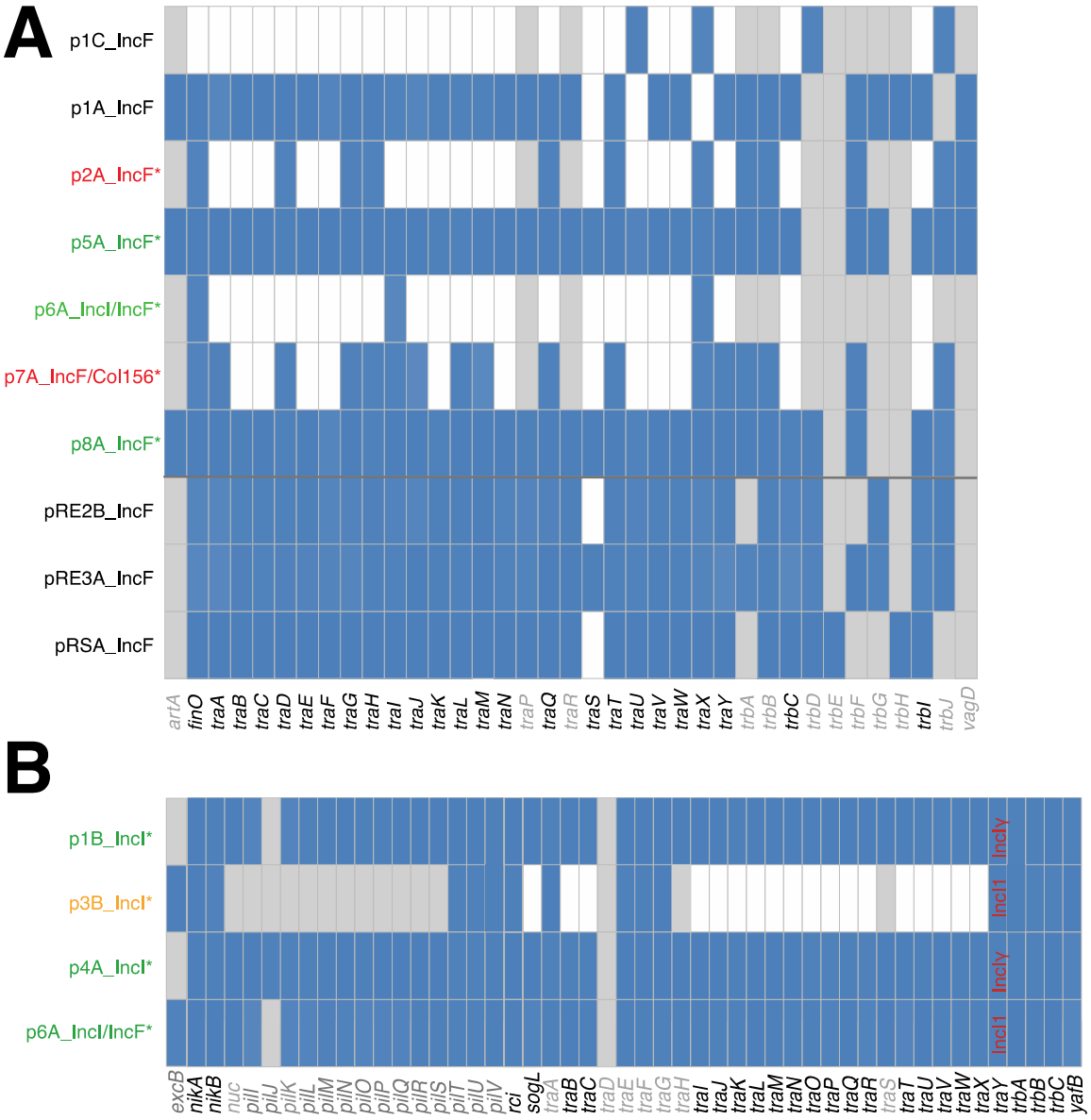
A
p1C_IncF
p1A_IncF
p2A_IncF*
p5A_IncF*
p6A_IncI/IncF*
p7A_IncF/Col156*
p8A_IncF*
pRE2B_IncF
pRE3A_IncF
pRSA_IncF
artA finO traA traB traC traD traE traF traG traH traI traJ traK traL traM traN traP traQ traR traS traT traU traV traW traX traY trbA trbB trbC trbD trbE trbF trbG trbH trbI trbJ vagD
B
p1B_IncI*
p3B_IncI*
p4A_IncI*
p6A_IncI/IncF*
IncIy
IncI1
IncIy
IncI1
excB nikA nikB nuc pilI pilJ pilK pilL pilM pilN pilO pilP pilQ pilR pilS pilT pilU pilV rci sogL traA traB traC traD traE traF traG traH traI traJ traK traL traM traN traO traP traQ traR traS traT traU traV traW traX traY trbA trbB trbC yafB

Supplementary Figures, Tables and Results

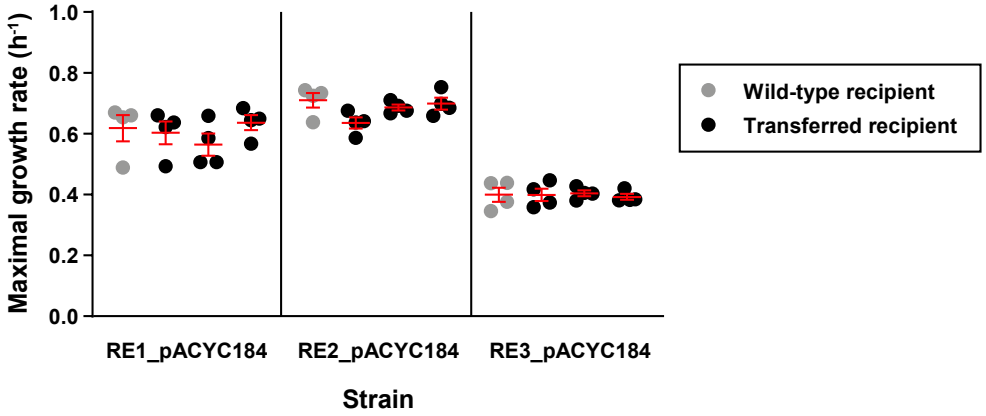

Figure S1. **Control for transconjugant growth rates.** We exposed recipients (RE1-RE3, *n = 4*) to the same culture handling as a conjugation assay would (black circles) to test for possible growth rate differences of recipients and transconjugants (Figure 5A-B) due to growth during the 1st generation conjugation experiment (see Materials and methods). Beams are mean values ± SEM.

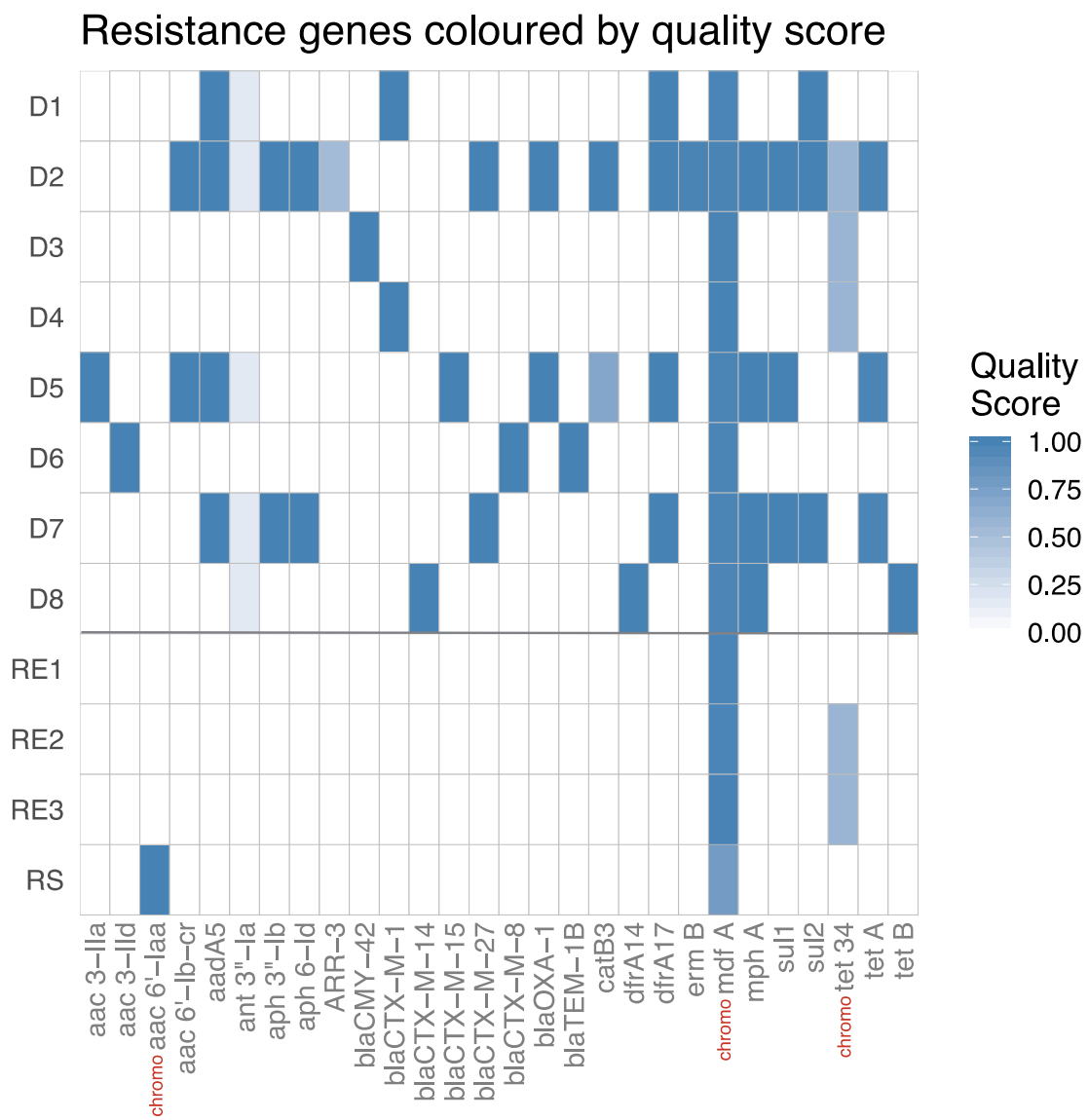

Figure S2 . Resistance genes. Presence (blue) or absence (white) of resistance genes in donors (D1-D8) and recipients (RE1-RE3, RS). The quality score q reflects the percent identity p and coverage c of the BLAST match to the listed genes, where $q = \frac{p}{100} \cdot \frac{c}{100}$. The genes ant 3''-Ia and ARR-3 were excluded from the S1 table. Chromosomal resistance genes are indicated with the red abbreviation chromo.

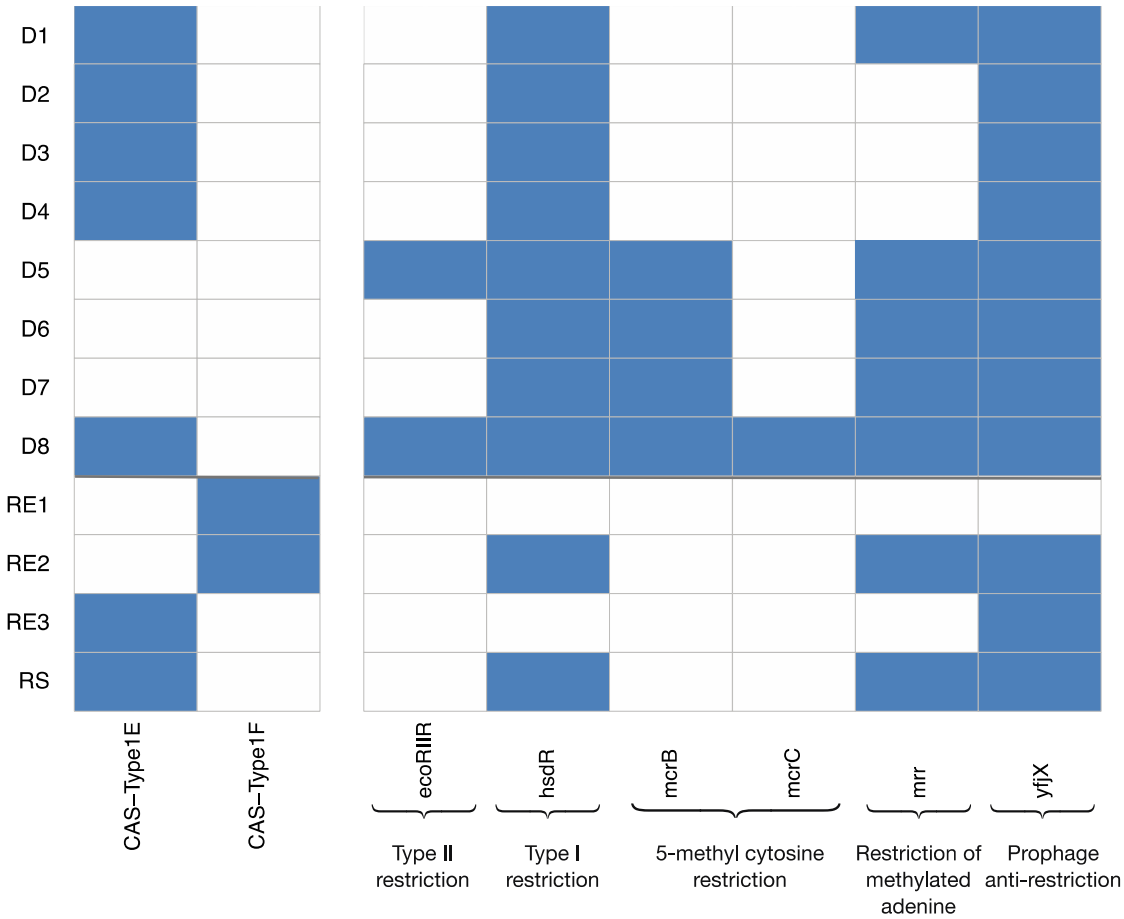

Figure S3 Bacterial immunity systems. Presence (blue) or absence (white) of CRISPR-Cas and restriction-modification systems (RM) in donors (D1-D8) and recipients (RE1-RE3, RS). CRISPR-Cas and RM systems were determined using prokka and confirmed using Rebase.

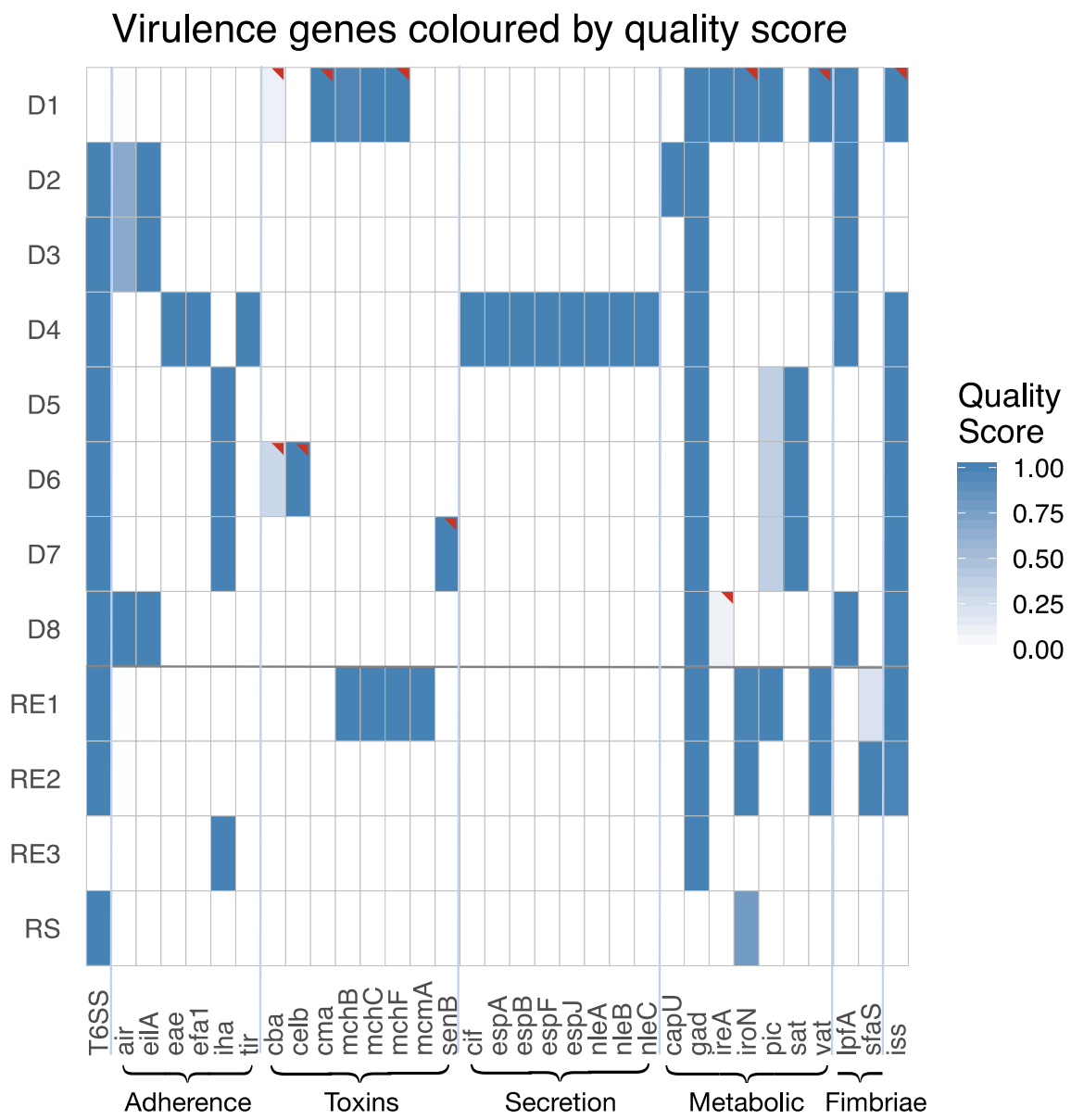

Figure S4 Type 6 secretion systems and virulence genes. Presence (blue) or absence (white) of Type 6 secretion systems (T6SS, defined by the presence of more than one prodigal T6SS-encoding gene in an operon) and virulence genes (found by BLAST) in donors (D1-D8) and recipients (RE1-RE3, RS). The quality score q reflects the percent identity p and coverage c of the BLAST match to the listed genes, where $q = \frac{p}{100} \cdot \frac{c}{100}$. Plasmid-based sequences are flagged with a red triangle. The only strain with a pathogenic virulence profile is D4, which carries chromosomally encoded intimin genes (*eae*, *tir*) commonly associated with Enteropathogenic *E. coli*. All strains except RE3 and D1, encode for a T6SS.

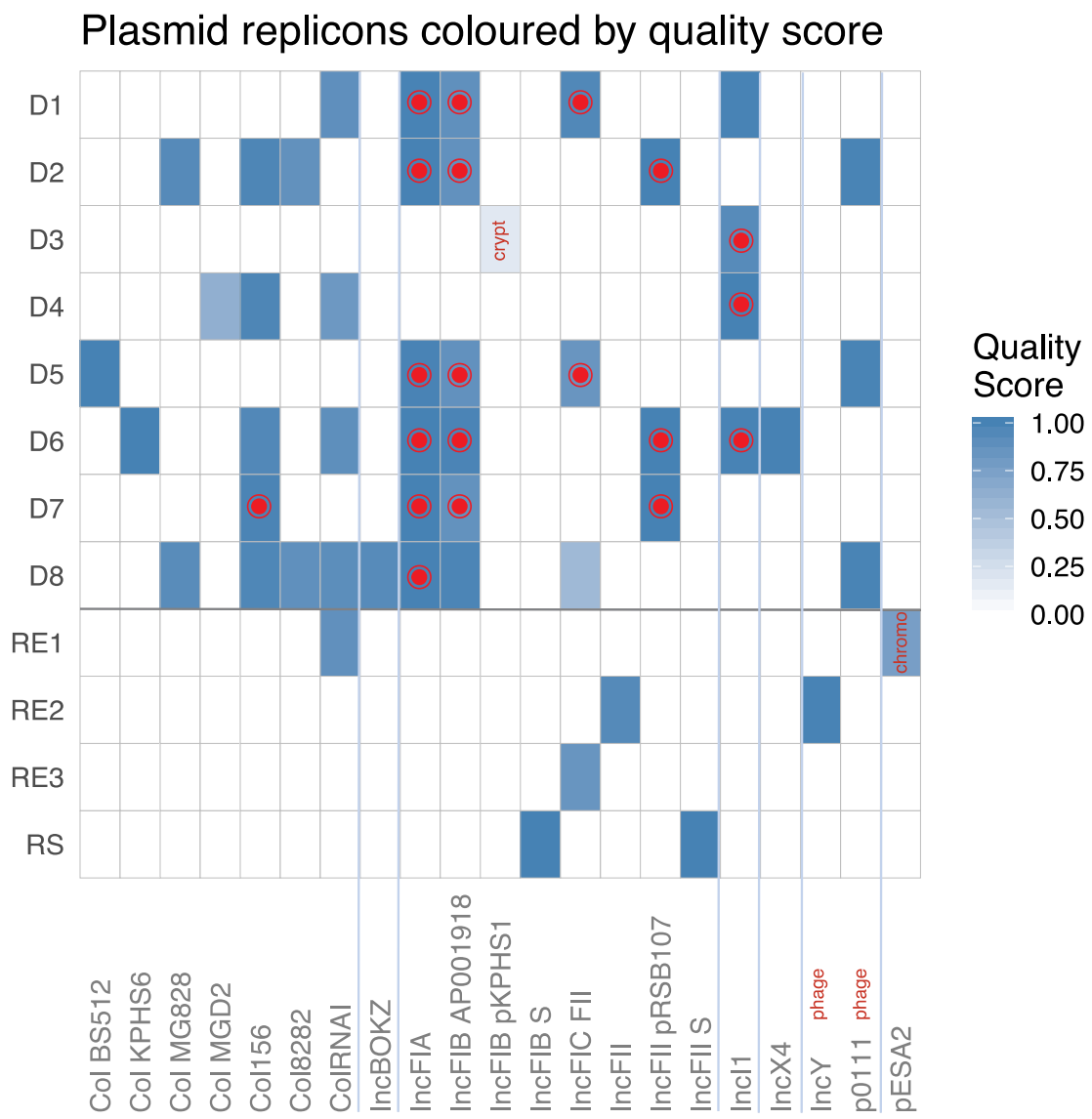

Figure S5 Plasmid replicons. Presence (blue) or absence (white) of plasmid replicons in donors (D1-D8) and recipients (RE1-RE3, RS). A red dot indicates the ESBL-plasmid, which can carry multiple replicons. The quality score q reflects the percent identity p and coverage c of the BLAST match to the listed genes, where $q = \frac{p}{100} \cdot \frac{c}{100}$. The matching regions of p3A_crypt and p8A_IncF were too short (< 75% coverage) to be included into S1 table. IncY and p0111 are P1-like phages.

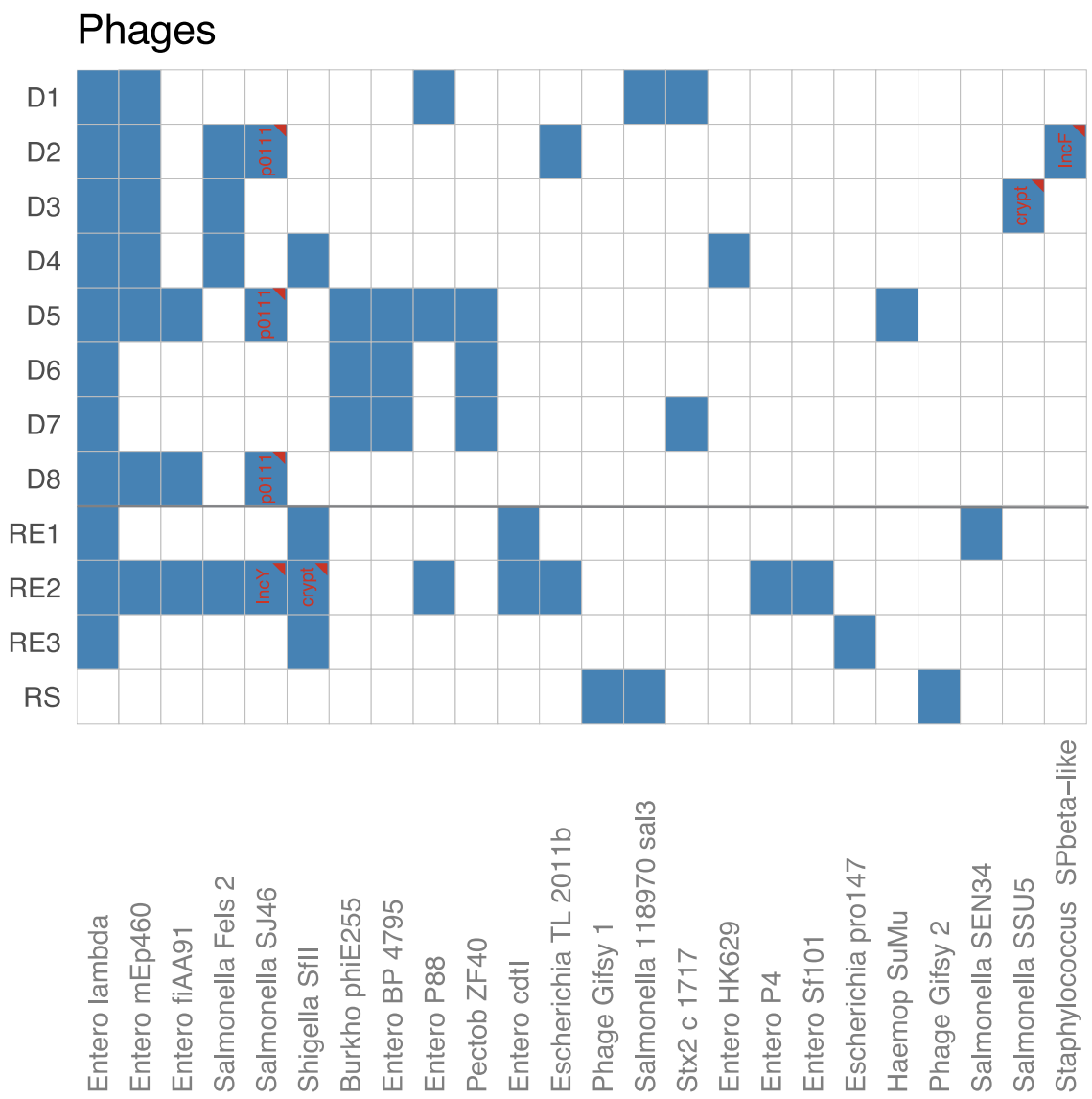

Figure S6 Phages. Presence (blue) and absence (white) of (pro)phages in donors (D1-D8) and recipients (RE1-RE3, RS). Plasmid-like phage sequences are flagged with a triangle and the replicon of the contig they were found on, both in red. All strains contain extensive (pro)phage related sequences.

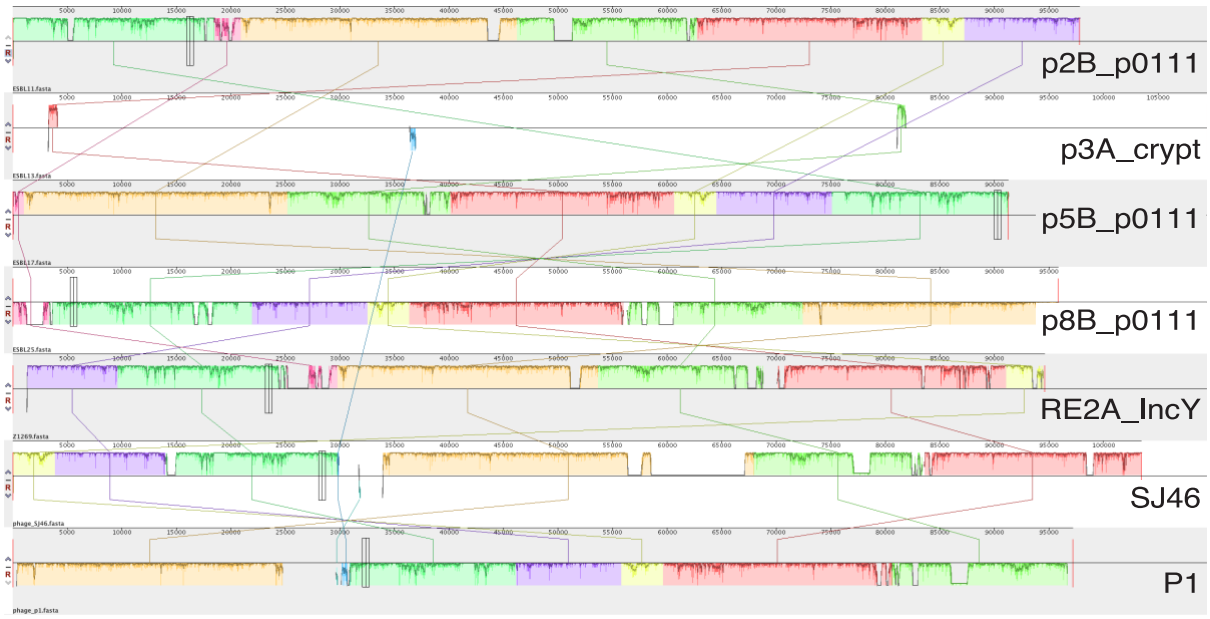

Figure S7 Mauve alignment. This alignment shows that the p0111 “plasmids” of D2, D5, D8, and the IncY “plasmid” of RE2 are highly related to each other and to the phages SJ46 and P1. Although highly similar to the phage SSU5, the p3A_crypt “plasmid” of D3 was largely unrelated to the P1-like phages.

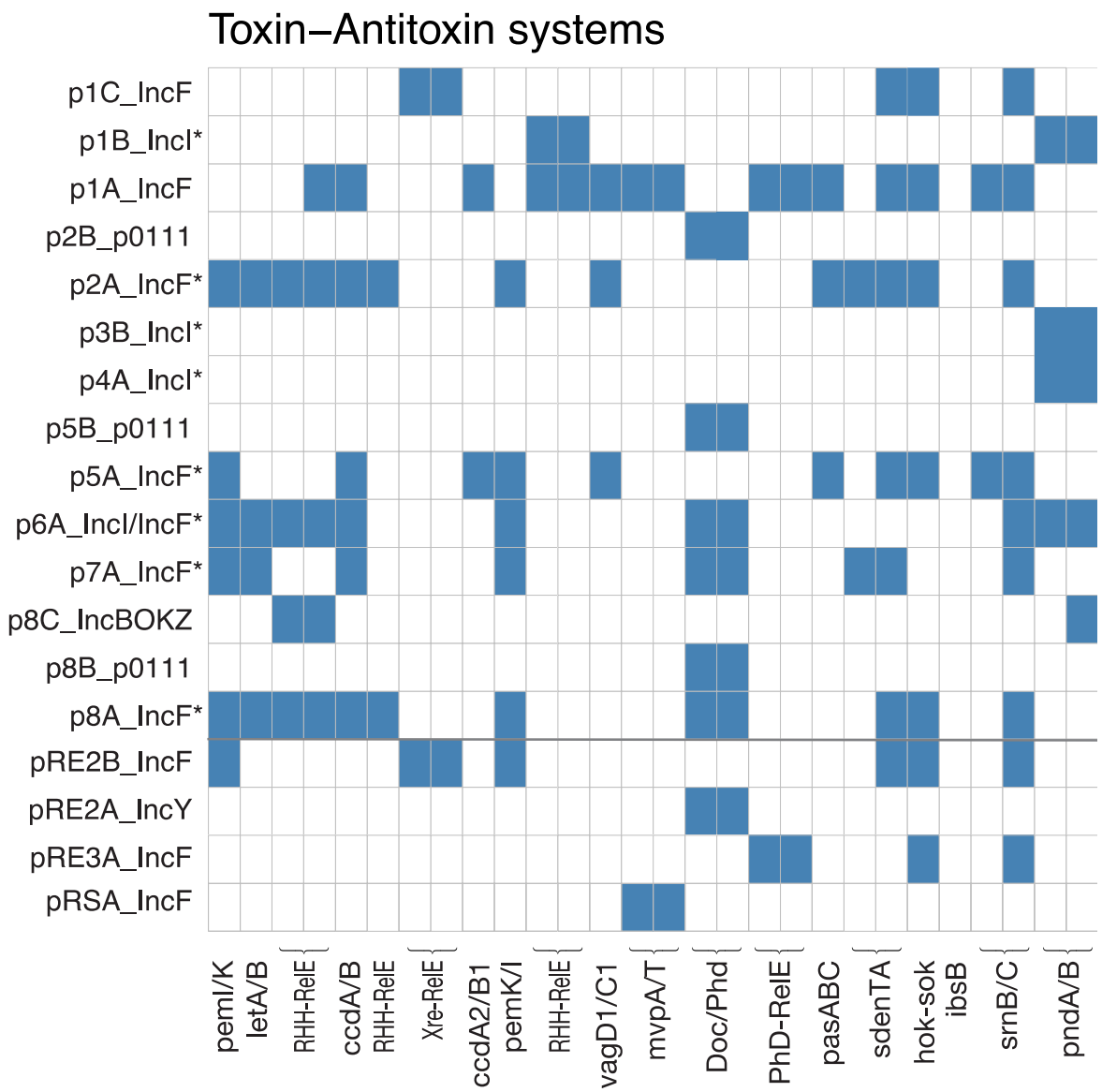

Figure S8 Toxin/Antitoxin-systems. Presence (blue) or absence (white) of Toxin/Antitoxin-systems (TA) in donors (D1-D8) and recipients (RE1-RE3, RS). Brackets indicate T/AT-pairs. The ESBL-plasmids are indicated by an asterisk. IncI1-plasmids and IncF-plasmids are generally associated with distinct TA-systems.

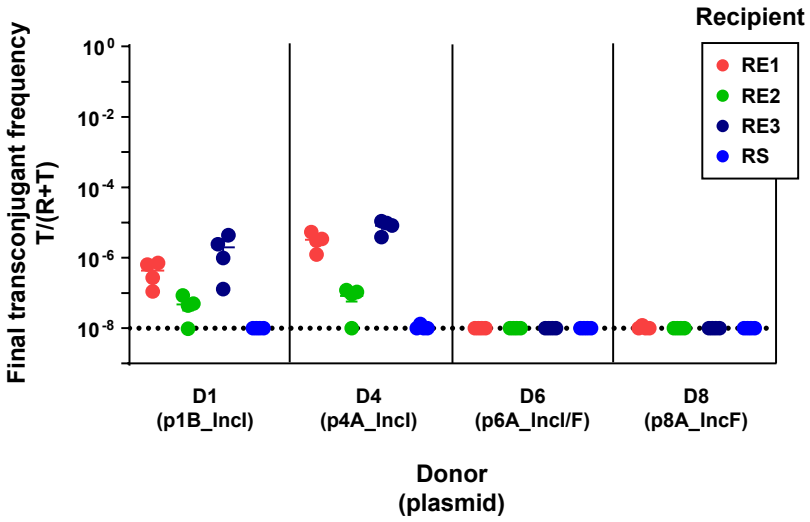

Figure S9 Surface-mating experiment. We allowed D1, D4, D6 and D8 to conjugate with all four recipients on LB-agar plates (*n = 4*). Resulting transconjugant frequencies depended on donor-plasmid pair and the recipient strain. Beams are mean values ± SEM, the dotted line indicates the detection limit by selective plating.

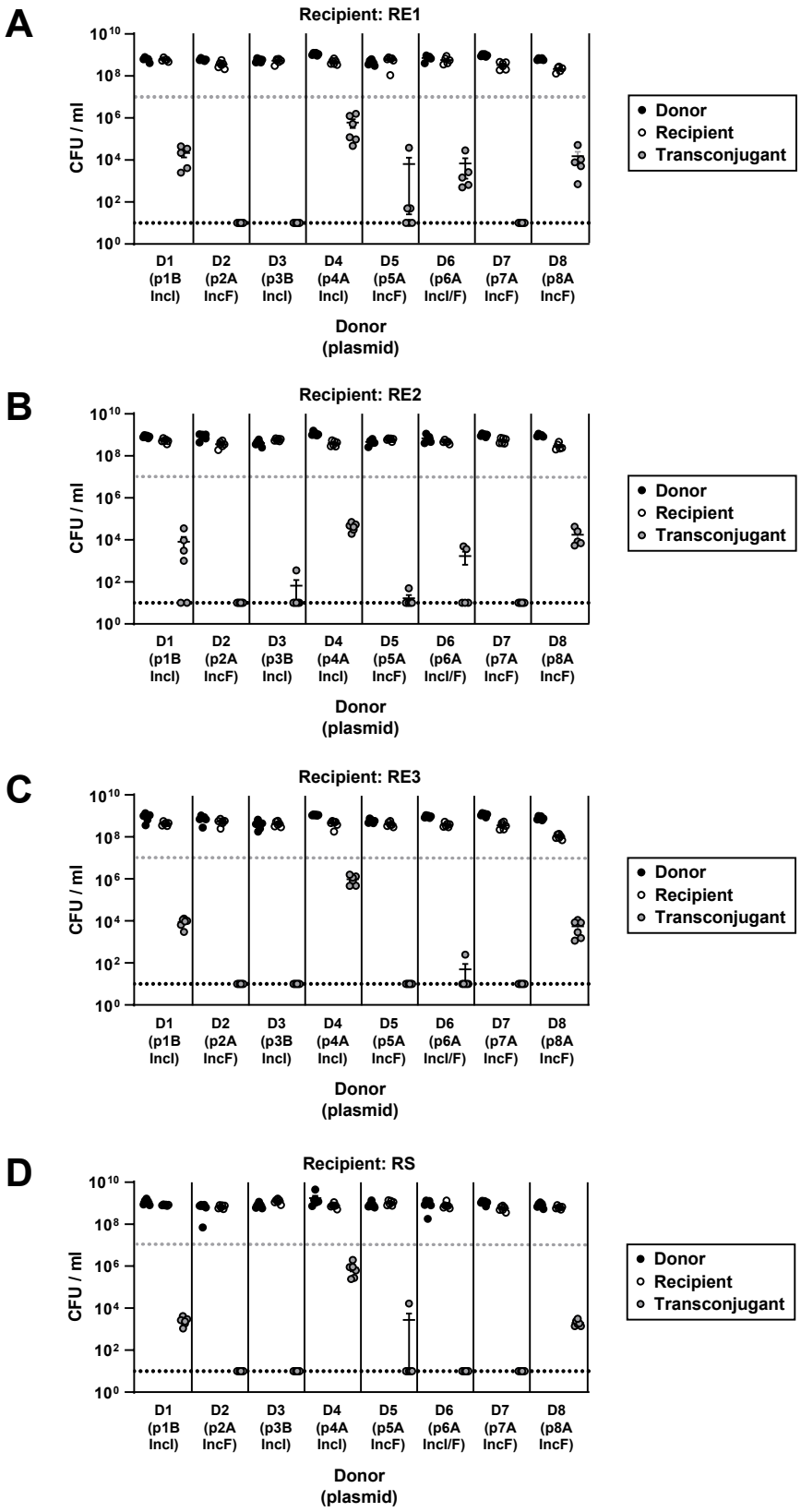

Figure S10 Absolute size of donor, recipient, and transconjugant populations in the 1st generation *in vitro* experiment. We performed conjugation experiments with natural donor-plasmid pairs and recipients RE1 (A), RE2 (B), RE3 (C) and RS (D). Beams are mean values ± SEM (*n = 6)*, dotted lines indicate the detection limit by selective plating, grey for donors and recipients, black for transconjugants.

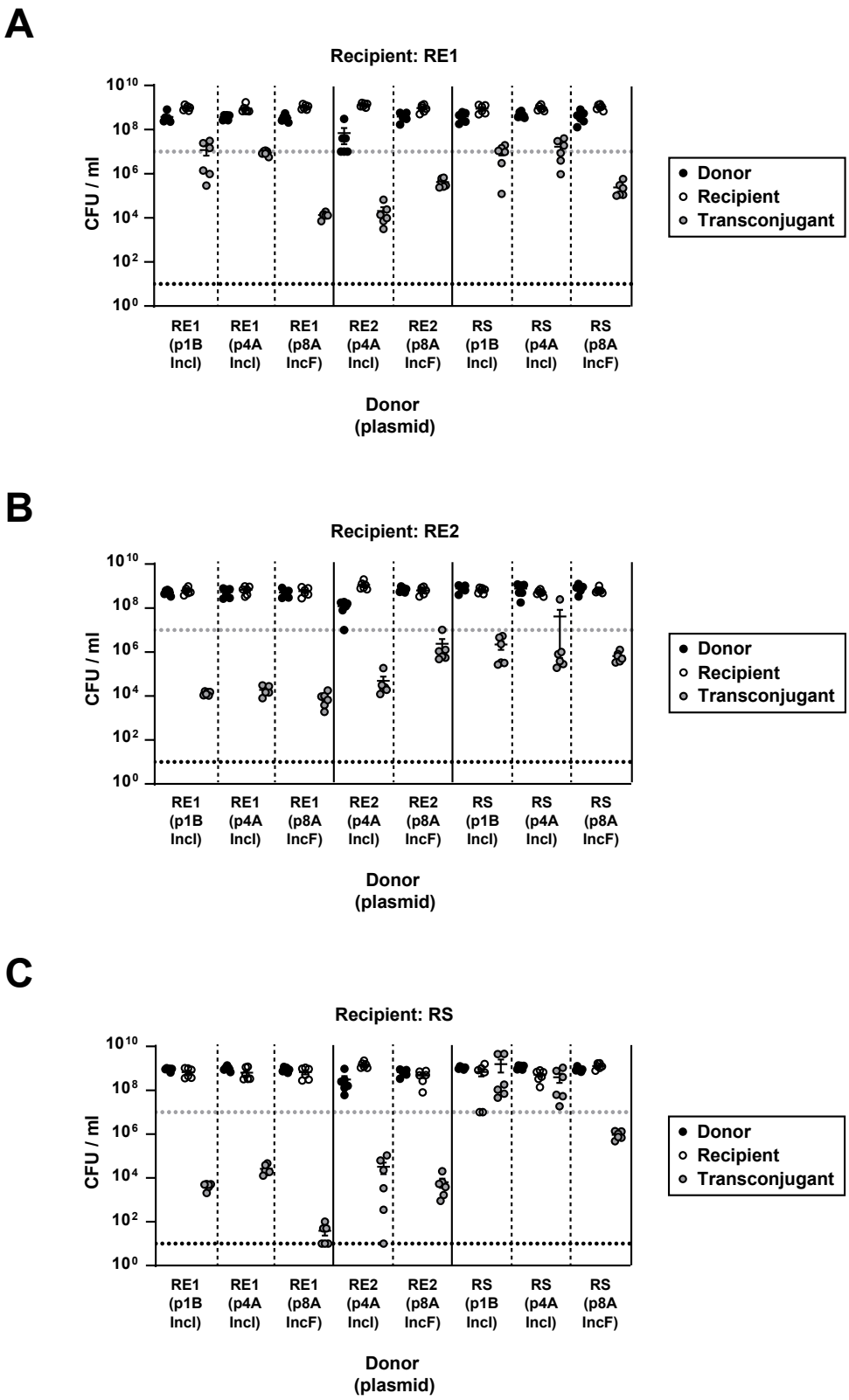

Figure S11 Absolute size of donor, recipient, and transconjugant populations in the 2nd generation *in vitro* experiment. We performed conjugation experiments with transconjugants from the 1st generation *in vitro* experiment as plasmid donors and recipients RE1 (A), RE2 (B,) and RS (C). Beams are mean values ± SEM (*n = 6*), dotted lines indicate the detection limit by selective plating, grey for donors and recipients, black for transconjugants.

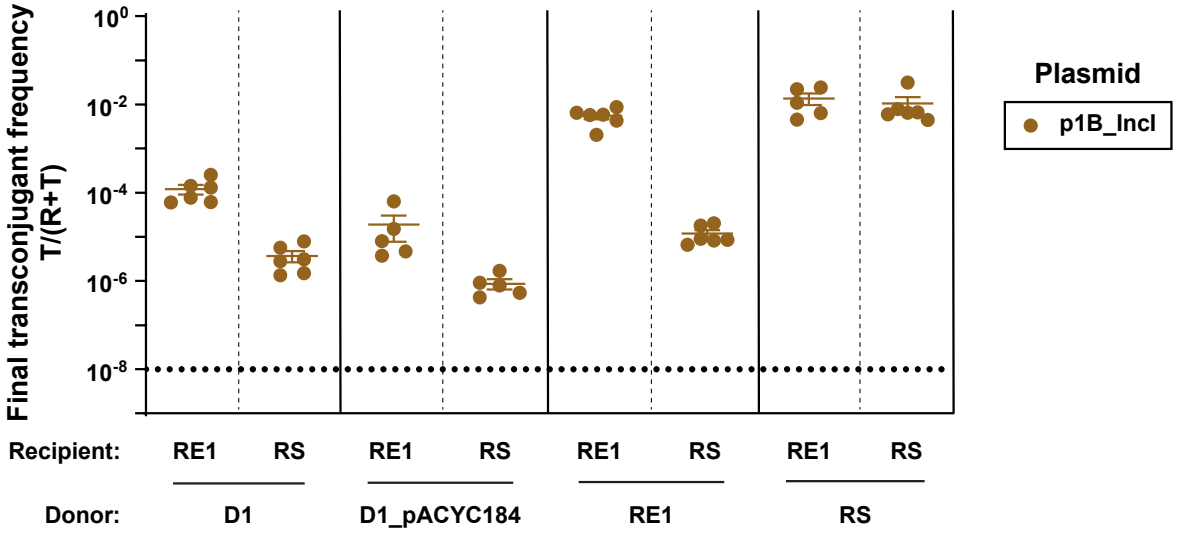

Figure S12 Plasmid transfer from native versus secondary host. We marked D1 with the same Cm-resistance plasmid (pACYC184) as the *E. coli* recipients in the 1st generation *in vitro* experiment, to exclude pACYC184 having a major effect on transconjugants' ability to donate plasmids. Indeed, pACYC184 in D1 had a significantly negative effect on transfer of p1B_IncI to RE1 (Wilcoxon Rank Sum Test, $P = 0.035$ after Holm's correction for multiple testing) and to RS (Student's t-Test, $P = 0.042$ after Holm's correction for multiple testing). Although significant, the effect of pACYC184 was small compared to the difference in transconjugant frequency that resulted from transfer from native versus 2nd generation donor strain. Circles represent independent replicates (*n = 5-6*) and the beams are mean values ± SEM. The detection limit was at ~10^{-8}.

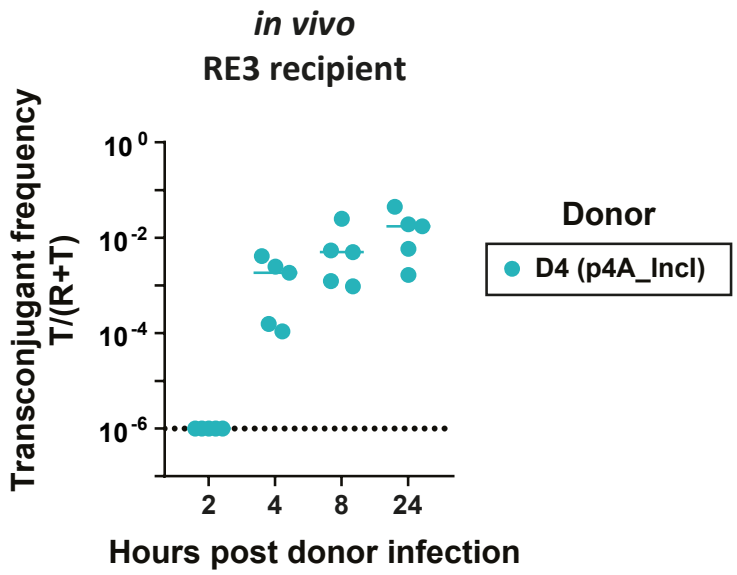

Figure S13 Rapid spread of p4A_IncI with recipient RE3. We monitored plasmid spread within the first 24 hours post donor infection. Plasmid spread is reported as final transconjugant frequency and enumerated in faeces by selective plating. The solid line indicates the median (*n = 5*), the dotted line indicate the detection limit for selective plating.

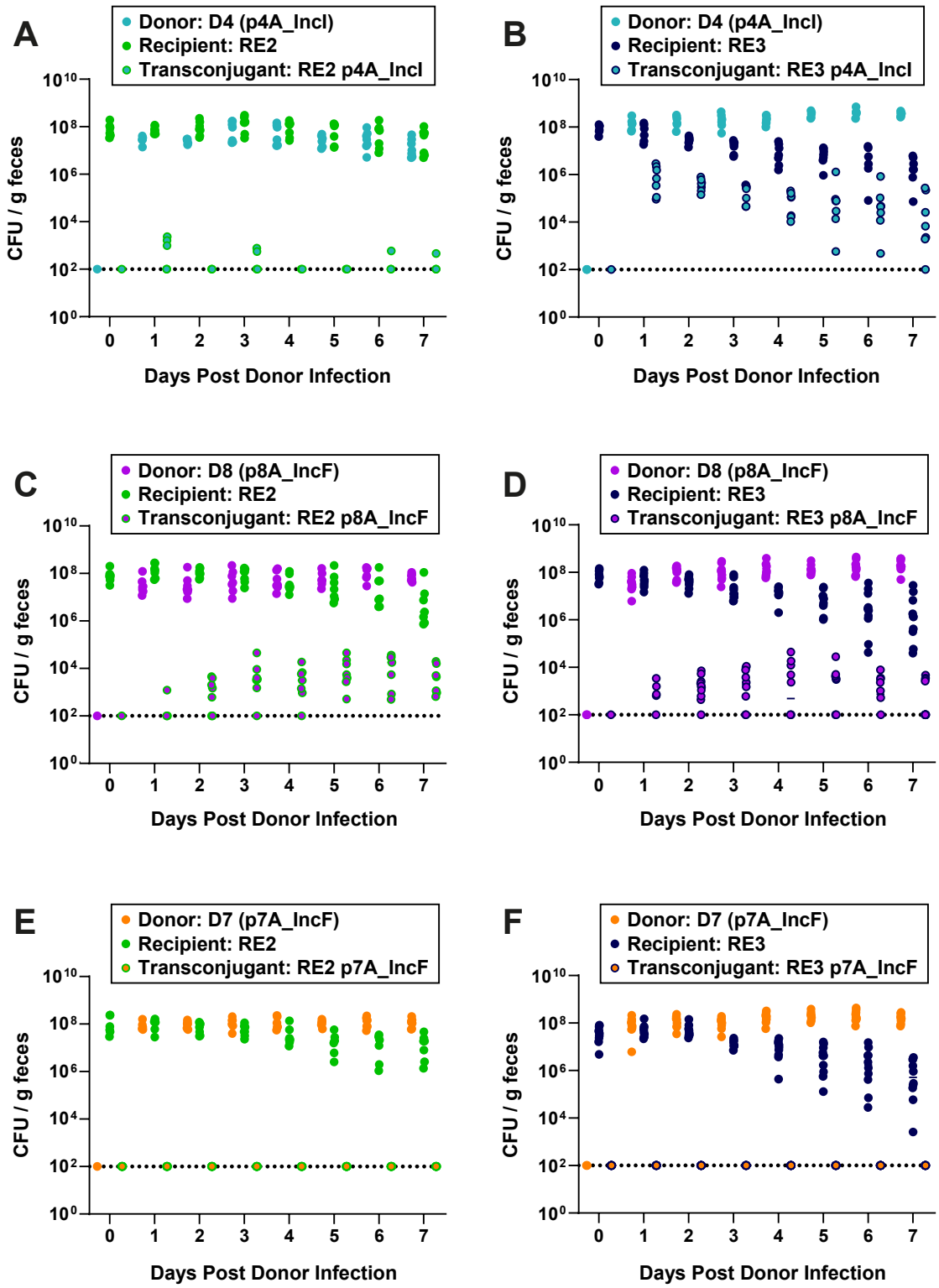

Figure S14 Total populations *in vivo*. Each panel reflects one donor-recipient pair and represents the population sizes of donors, recipients, and transconjugants in Fig. 4. A) Conjugation from D4 to RE2 (*n = 7*). B) Conjugation from D4 to RE3 (*n = 7*). C) Conjugation from D8 to RE2 (*n= 7*). D) Conjugation from D8 to RE3 (*n = 10*). E) Conjugation from D7 to RE2 (*n = 7*). F) Conjugation from D7 to RE3 (*n = 10*). The dotted line indicates the detection line by selective plating. The solid lines indicate the median.

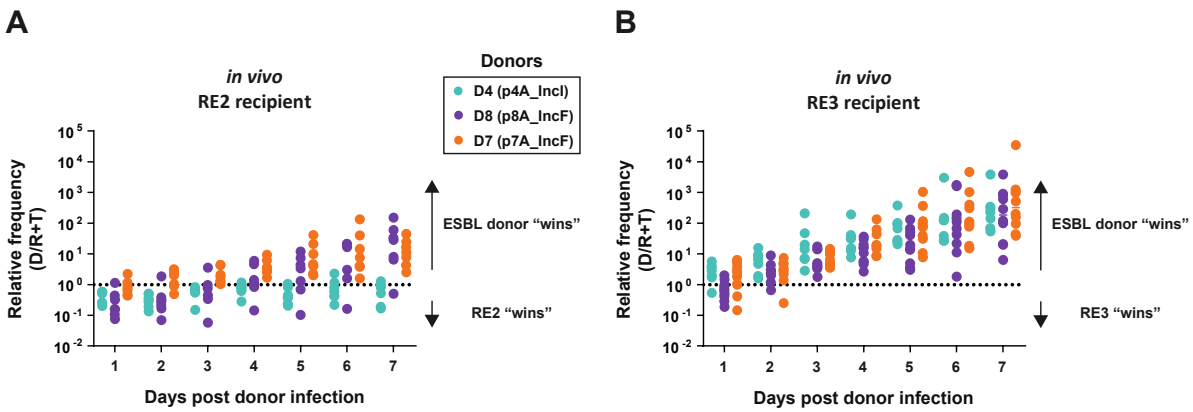

Figure S15 Direct competition between donors and recipients *in vivo.* We performed competition experiments by colonizing the mice with a 1:1 mix of plasmid donors with RE2 (A) (*n=7*) or RE3 (B) (*n=7* for D4-RE3; *n=10* for D8-RE3 and D7-RE3). The relative frequency was calculated by dividing the recipient population by the donor strain population.

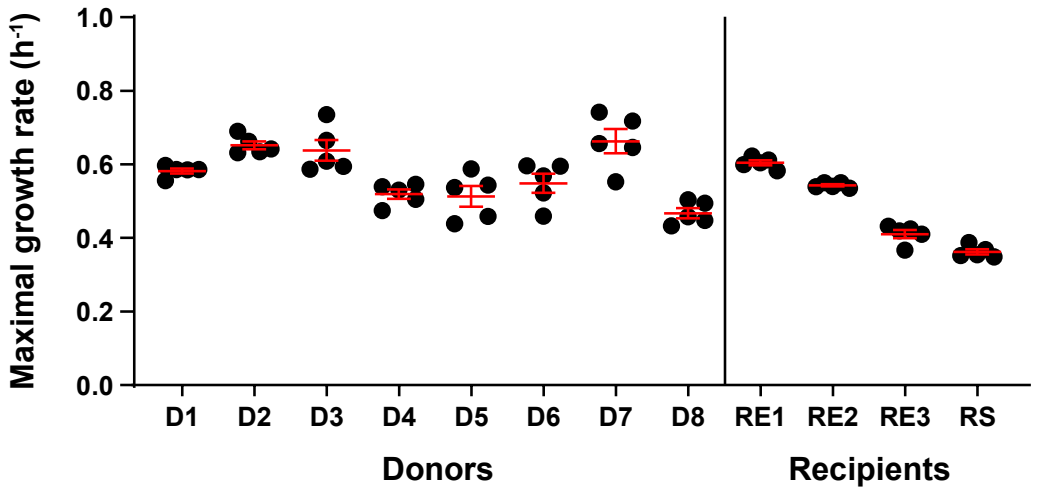

Figure S16 Maximal growth rates of donors and recipients used in the 1st generation *in vitro* experiment. Growth rates were estimated using OD measurements over 24 hours (*n=5*) in the absence of antibiotics.

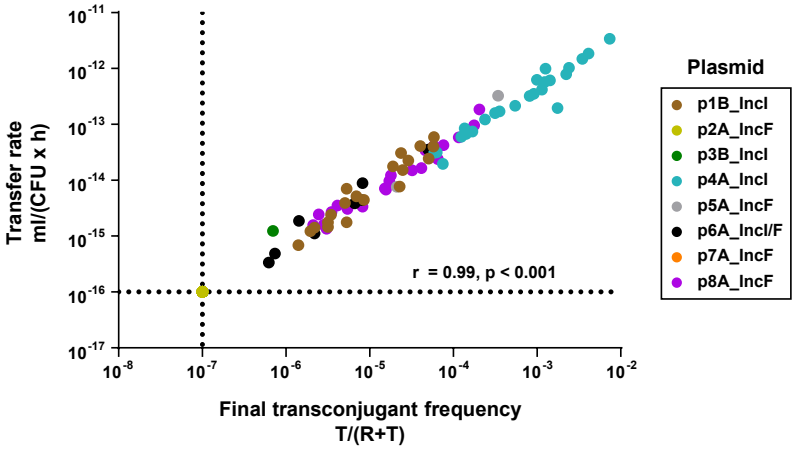

Figure S17 Correlation of plasmid transfer rate and final transconjugant frequency estimated using the Simonsen method. Each data point results from the same liquid mating culture shown in Fig 2. Transconjugant frequencies and transfer rates can be found in the S3 Table**.**

Supplementary Tables

Table S1 Strain overview. Table S1 is a separate file. Overview of all strains used in this study, including their sequence type (ST), natural plasmid content and detected resistance genes. Replicon and resistance gene hits are only shown in this table if they had a coverage and percent identity of at least 70%, leading to a few differences with respect to Figures S2 and S5, most notably IncFIC_FII in D8. Contiguous sequences (contigs) were denoted "c" or "p" for chromosomal or plasmid, respectively. Short sequences (up to 5 kB) that mapped to the own chromosome, and any contigs smaller than 1kB were removed. Any remaining contigs without a known replication gene were denoted "_crypt" for cryptic.

Table S2 Overview of plasmid transferring and mutations accumulating during conjugation experiments. Table S2 is a separate file.

Table S3 Phenotypic resistance profile of donor strains. Minimum inhibitory concentration (µg/mL) measurements of ESBL donors used in this study. The ESBL-resistance phenotype was defined by resistance to Ceftriaxone and Ceftazidime.

Strain	Amp	Amo/C	Pip-T	Ceftaz	Ceftri	Cefe	Erta	Imi	Mero	Tobra	Amika	Cotri	Cipro	Coli
D1	>=32	4	<=4	<=1	32	2	<=0.5	<=0.25	<=0.25	<=1	<=2	>=320	<=0.25	<=0.5
D2	>=32	>=32	8	4	32	2	<=0.5	<=0.25	<=0.25	>=16	4	>=320	>=4	<=0.5
D3	>=32	>=32	>=128	>=64	>=64	>=64	<=0.5	<=0.25	<=0.25	>=16	>=64	>=320	>=4	<=0.5
D4	>=32	8	<=4	<=1	>=64	<=1	<=0.5	<=0.25	<=0.25	<=1	<=2	<=20	<=0.5	<=0.5
D5	>=32	16	8	16	>=64	>=64	<=0.5	<=0.25	<=0.25	>=16	16	>=320	>=4	<=0.5
D6	>=32	4	<=4	<=1	>=64	>=64	<=0.5	<=0.25	<=0.25	8	<=2	<=20	>=4	<=0.5
D7	>=32	4	<=4	4	>=64	4	<=0.5	<=0.25	<=0.25	<=1	<=2	>=320	>=4	<=0.5
D8	>=32	4	4	<=1	>=64	<=1	<=0.5	<=0.25	<=0.25	<=1	<=2	>=320	<=0.25	<=0.5

Abbreviations: **Amp** = Ampicillin; **Amo/C** = Amoxicillin/Clavulanic acid; **Pip-T** = Piperacillin-Tazobactam; **Ceftaz** = Ceftazidime; **Ceftri** = Ceftriaxone; **Cefe** = Cefepim; **Erta** = Ertapenem; **Imi** = Imipenem; **Mero** = Meropenem; **Tobra** = Tobramycin; **Amik**a = Amikacin; **Cotri** = Cotrimoxazol; **Cipro** = Ciprofloxacin; **Coli** = Colistin. Interpretatin of MIC breakpoints according to EUCAST guidelines (v8.1).

Table S4 Priors for the phylogenetic tree inference. Parameter priors for the birth-death tree prior.

Become Uninfectious Rate	LogNormal (mu = 0, sigma = 1)
Kappa	LogNormal (mu = 1.5, sigma = 1.25)
Origin	LogNormal (mu = 6, sigma = 1.25)
Reproductive Number	LogNormal (mu = 0, sigma = 1)
Sampling Proportion	Beta (alpha = 1.2, beta = 10)

Supplementary Results

Growth rates of all strains in the 1st generation *in vitro* experiments

To calculate whether the mean difference in growth rate between recipients and transconjugants alone could explain the observed final transconjugant frequencies (Figure 2), we calculated the final transconjugant frequency that would result from such a purely clonal expansion. To simplify the calculation, we assumed exponential growth of the recipient and transconjugant population, starting from $R(0)$ and a single individual $T(0)=1$ respectively. Using these assumptions, one can calculate the minimal transconjugant growth rate ψ_T needed to explain the final transconjugant frequency after 24 hours (f) :

$$\psi_T > \psi_R - \frac{1}{24}\ln\left(\frac{\frac{1}{f}-1}{R(0)}\right) \quad (1)$$

Here ψ_R is the corresponding plasmid-free recipient growth rate.

Measured populations growth rates of recipients and transconjugants. The data is the same as in the plasmid cost comparison (Figure 5A/B) and stems from manual OD measurements over 24 hours (*n = 12*). Note that these absolute growth rates differ from the ones estimates for Figures S1 and S16 (See Materials and methods).

	RE1_pACYC184	RE2_pACYC184	RE3_pACYC184	RS_marTcat
- (recipient)	0.96 ± 0.01	0.98 ± 0.01	0.66 ± 0.006	0.34 ± 0.002
with p1B_IncI	0.99 ± 0.01	-	-	**0.38** ± 0.009
with p4A_IncI	0.95 ± 0.01	0.95 ± 0.01	0.70 ± 0.006	0.37 ± 0.001
with p8A_IncF	0.88 ± 0.004	0.99 ± 0.006	0.67 ± 0.004	**0.38** ± 0.0003

Calculated minimal transconjugant growth rates needed to explain the observed final transconjugant frequencies (Figure 2).

	RE1_pACYC184	RE2_pACYC184	RE3_pACYC184	RS_marTcat
with p1B_IncI	1.07	1.06	0.75	**0.36**
with p4A_IncI	1.23	1.16	0.96	0.60
with p8A_IncF	1.10	1.13	0.80	**0.36**

In two cases, i.e. transconjugant RS carrying p1B_IncI and p8A_IncF, the measured growth rate of transconjugants was greater than the calculated minimal growth rate needed to explain the observed final transconjugant frequencies. Thus, for these two out of the 10 donor-recipient combinations (excluding RE2 and RE3 carrying p1B_IncI), we cannot exclude that final transconjugant frequencies were reached by clonal expansion, rather than conjugative transfer. Our calculations, however, are conservative, because of the assumption of exponential growth, which overestimates the number of transconjugants that could have resulted from clonal expansion.